The Pennsylvania State University
**APPLIED RESEARCH LABORATORY**
P.O. Box 30
State College, PA 16804

# SIMULTANEOUS, BIDIRECTIONAL FIBER OPTIC DATA LINK FOR AN AUTONOMOUS UNDERWATER VEHICLE

by

J. C. Young



Technical Report No. TR 93-13
November 1993

Supported by:
Office of Naval Research

L.R. Hettche, Director
Applied Research Laboratory

# REPORT DOCUMENTATION PAGE

Form Approved
OMB No. 0704-0188



| 1. AGENCY USE ONLY (Leave blank) | 2. REPORT DATE | 3. REPORT TYPE AND DATES COVERED |
|---|---|---|
| | November 1993 | |

**4. TITLE AND SUBTITLE**

Simultaneous, Bidirectional Fiber Optic Data Link
Autonomous Underwater Vehicle

**5. FUNDING NUMBERS**

N00039-92-C-0100

**6. AUTHOR(S)**

J. C. Young

**7. PERFORMING ORGANIZATION NAME(S) AND ADDRESS(ES)**

Applied Research Laboratory
The Pennsylvania State University
P.O. Box 30
State College, PA 16804

**8. PERFORMING ORGANIZATION REPORT NUMBER**

TR-93-13

**9. SPONSORING/MONITORING AGENCY NAME(S) AND ADDRESS(ES)**

Office of Naval Research
800 North Quincy Street
Arlington, VA 22217-5660

**10. SPONSORING/MONITORING AGENCY REPORT NUMBER**

**11. SUPPLEMENTARY NOTES**

**12a. DISTRIBUTION/AVAILABILITY STATEMENT**

Unlimited

**12b. DISTRIBUTION CODE**

**13. ABSTRACT** *(Maximum 200 words)*

Autonomous Underwater Vehicles (AUVs) are currently in use for acoustic research. The physical size and weight of its on-board electronic equipment and power supplies hinder the AUV. To take advantage of the large amount of space available on the AUV's launch craft, and "umbilical"-type link between the AUV and its launch craft was designed. This link enables the data processing and recording electronics to be moved from the AUV to the launch craft. The removal of the electronics reduces the weight and possibly the size of the AUV, and it reduces system power requirements. A copper wire link is impractical because it does not have the required bandwidth and it reduces mobility and restricts vehicle separation from the surface-based launch craft. As such, a fiber optic data link was selected to link the AUV to the launch craft. This link was designed so that all data recording and processing are accomplished on the launch craft, while maintaining the mobility and separation capabilities of the original autonomous vehicle. The link was designed to fit into an existing vehicle with minor mechanical modifications.

| 14. SUBJECT TERMS | 15. NUMBER OF PAGES |
|---|---|
| UUV, fiber optic, data, link | 97 |
| | 16. PRICE CODE |

| 17. SECURITY CLASSIFICATION OF REPORT | 18. SECURITY CLASSIFICATION OF THIS PAGE | 19. SECURITY CLASSIFICATION OF ABSTRACT | 20. LIMITATION OF ABSTRACT |
|---|---|---|---|
| UNCLASSIFIED | UNCLASSIFIED | UNCLASSIFIED | UNLIMITED |

# ABSTRACT

Autonomous Underwater Vehicles (AUVs) are currently in use for acoustic research. The physical size and weight of its on-board electronic equipment and power supplies hinder the AUV. To take advantage of the large amount of space available on the AUV's launch craft, an "umbilical"-type link between the AUV and its launch craft was designed. This link enables the data processing and recording electronics to be moved from the AUV to the launch craft. The removal of the electronics reduces the weight and possibly the size of the AUV, and it reduces system power requirements. A copper wire link is impractical because it does not have the required bandwidth and it reduces mobility and restricts vehicle separation from the surface-based launch craft. As such, a fiber optic data link was selected to link the AUV to the launch craft. This link was designed so that all data recording and processing are accomplished on the launch craft, while maintaining the mobility and separation capabilities of the original autonomous vehicle. The link was designed to fit into an existing vehicle with minor mechanical modifications. The purpose here is to document the development and design efforts of incorporating a fiber optic data link into an AUV for use in underwater applications.

# TABLE OF CONTENTS

# LIST OF FIGURES

# LIST OF TABLES

# GLOSSARY OF FIBER OPTIC TERMS

APD (avalanche photodiode)
: A photodetector that uses the avalanche multiplication effect to increase the output photocurrent.

BER (bit error rate)
: The number of erroneous bits received divided by the number of bits transmitted. A measure of performance in optical systems.

Biconic
: A bayonet type of fiber optic connector.

DFB (distributed feedback)
: A type of laser using Bragg reflectors or periodic gratings to obtain lasing action.

Fabry-Perot
: A type of laser using mirrors to obtain a lasing action.

LED (light emitting diode)
: A p-n junction semiconductor device that produces light through spontaneous emission.

Manchester
: A type of data encoding scheme used in optical systems.

NRZ (non return to zero)
: A data format that does not have a transition for every clock cycle.

PIN (positive intrinsic negative)
: A junction photodiode that changes its electrical conductivity in accordance with its incident light.

rx
: The fiber optic receiver.

RZ (return to zero)
: A data format that has a transition during every clock cycle.

SMA
: A threaded type of fiber optic connector.

SNR (signal to noise ratio)
: The power to noise ratio at the input of an optical receiver.

ST
: A bayonet type of fiber optic connector.

tx
: The fiber optic transmitter.

WDM (wavelength division multiplexer)
: Device used to multiplex two or more signals on an optical fiber.

# Chapter 1

# INTRODUCTION

For many years, copper media has been the information transmission means of choice. This media has served the communication market very well, but technological advances have dictated an increase in the rate of data transmission and sparked the desire for greater transmission capacity. The use of optical fiber as a replacement for copper media is proving to be an irresistible force for handling the enormous amounts of information that must be transmitted across the country and around the world. The field of fiber optics is quickly emerging as the technology of today and tomorrow.

Fiber optics transmission is basically the transmission of information from one point to another using a thin strand of glass or plastic, called an optical fiber, as the transmission medium. The optical fiber functions in a manner similar to the copper wire, but it offers the following advantages (Sterling 1987):

Wide Bandwidth -- Optical fibers have a potential useful range of up to about 1 THz, compared to less than 100 MHz for copper media.

Low Loss -- For frequencies up to $10^8$ Hz, loss in an optical fiber is consistently less than 5 $\frac{dB}{km}$. Losses in copper cables increase with frequency. These losses range from 6 $\frac{dB}{km}$ at frequencies less than 1 MHz to losses greater than 30 $\frac{dB}{km}$ for frequencies greater than 10 MHz.

Electromagnetic Immunity -- Optical fibers do not pick up or radiate electromagnetic interference (EMI). Copper cables, on the other hand, are very susceptible to EMI. In some cases, the EMI in copper cables is so severe that the transmitted signal is distorted or even lost.

Security -- Fiber optics does not radiate any energy and is extremely difficult to tap. Copper cables radiate energy that can be picked up by sensitive antennas and translated to the original transmitted signal.

Light Weight -- A fiber optic cable with the same information-carrying capability as its copper counterpart weighs far less. A single-conductor optical cable weighs 9 lb/1000 ft; a comparable copper cable weighs 80 lb/1000 ft.

Small Size -- An optical fiber is almost ten times smaller than its copper counterpart; in most cases, a single fiber can replace several copper conductors due to its higher bandwidth and multiple information-carrying capabilities.

The interest in optical communications arose in 1960 with the development of the laser. The initial activity concentrated on experiments using atmospheric optical channels, since early fibers had extremely large attenuation losses of more than 1000 dB/km. By 1970, however, the attenuation was reduced to as low as 20 dB/km, and by the late 1970's, fiber attenuation as low as 2 dB/km was achieved.

The use of optical fibers for transmission became widespread during the 1980's, evidenced by the installation of the fiber optic telecommunication networks throughout the world. The trend is continuing into the 1990's, made apparent by the recent change of coaxial cables to optical fibers for analog video distribution. Optical fibers are also replacing copper media in telephone systems and computer networks. It is predicted that by the year 2010, over $200 billion in fiber optic systems will be installed and that the majority of the communication traffic will be fiber optic (Weik 1989; Agrawal 1992).

Although the use of optical fibers is prevalent in transmission networks, the use of fiber optic technology is not widespread in applications involving autonomous underwater vehicle (AUV) communication and control. Current copper media links have very low bandwidth and restrict the vehicle's mobility and separation capabilities from its launch craft. The objective of this thesis is to document the underwater application of fiber optic technology to help alleviate the physical constraints in an AUV.

The physical limitations of an AUV have dictated moving some electronics from the AUV to its launch craft to take advantage of the available space. An "umbilical"-type link between the AUV and launch craft allows for the removal of the data processing and recording electronics from the AUV. This link allows the vehicle to maneuver through volumes of water collecting acoustic research data, while the acoustic data is both processed and recorded on the launch craft. The data processing results in steering commands that direct the vehicle toward various sources. To satisfy the umbilical need, an optical fiber was chosen as the transmission medium. Fiber optics offers simultaneous, bidirectional transmission capabilities and provides for future system

upgrades. Optical fiber technology has yet to reach its full potential, while copper wire transmission has, for the most part, reached its peak and is being replaced by optical fibers.

The purpose of the umbilical fiber optic link is to provide simultaneous, bidirectional communication between the underwater vehicle and its launch craft. The advantages of the link are two-fold. First, the data processing and recording equipment and their respective power supplies can be removed from the vehicle and placed on the launch craft. This reduces the weight and possibly the size of the vehicle. This also provides for increased data processing capabilities because of the large amount of space available on the launch craft. Second, the reduction in size and weight results in a reduced power demand and allows for increased experiment duration. To be effective, the link must possess the characteristics currently offered by the original autonomous vehicle, i.e. mobility and separation from the launch craft, and satisfy the following key objectives:

- simultaneous bidirectional communication capability
- transmission distances limited to 20 km due to available fiber spool sizes
- minimal mechanical changes to current vehicle
- off-board record capability
- off-board data processing capability

This thesis presents the fiber optic data link design and development efforts and provides descriptions of the tests performed to verify achievement of the design objectives.

# Chapter 2

## THEORY FOR THE DESIGN OF THE FIBER OPTIC DATA LINK

The design of an optical link involves the interrelationship of its components, of which the fiber, the transmitter, and the receiver are most important. The actual design of the link may require several iterations before desired performance levels are satisfied. The components for the link must be carefully selected or designed by considering their characteristics with respect to system performance.

In planning a fiber optic system, the key application requirements must first be established so that components can be selected. These requirements involve the data rates, the transmission distances, and the desired bit error rate (BER).

The distance limit between the fiber optic transmitter and receiver is determined by the source power, the fiber losses, and the receiver sensitivity. Receiver sensitivity is a function of both the data rate and the required BER. To fulfill the design requirements, the choices for the following components of the fiber optic system can be evaluated.

- fiber type
- operating wavelength
- transmitter type
- receiver type
- modulation code
- connectors
- mechanical concerns

Two analyses are usually carried out to ensure that the desired system requirements are met. These are the link power budget and the rise time budget analyses.

## 2.1 Link Power Budget

The power budget provides a convenient method of analyzing and quantifying the losses incurred in a fiber optic link. The budget is the difference between the transmitter power and the receiver sensitivity. This budget must be able to accommodate the summation of all system losses.

In approaching a design, the first parameter to be selected is the wavelength(s) of operation. By first selecting the wavelength, the number of active components to be selected is reduced by about 50 percent (Keiser 1983, Killen 1991). For distances less than 1 km, the preferred wavelength is 800 nm. Step-index or graded-index multimode fibers can be used with a light emitting diode (LED) source for most applications up to 2 km. A laser diode source may be required for higher data rates. A longer wavelength provides both a higher maximum data rate and longer distance at low data rates.

For links between 1 and 5 km, a laser in the 800 nm window or an LED in the 1300 nm window can be used. For distances greater than 10 km, a laser source and a single-mode fiber are required, and a wavelength of 1300 nm is preferred. Distances upward of 25 km require a wavelength of 1550 nm with dispersion-shifted single-mode fiber. Laser sources can be used with both single-mode and multimode fiber. An LED source can only be used with multimode fiber.

There are three basic fiber types: multimode step-index, multimode graded-index, and single-mode step-index. The attenuation (loss) in the fiber varies with the fiber type. In a step-index fiber, light rays reflect off the core boundary and travel in a zig-zag fashion down the fiber core. In a graded-index fiber, they refract and travel in a sinusoidal fashion down the fiber core (Lacy 1982).

The index-profile is the parameter used to classify the fiber. The index-profile refers to how the refractive index of the fiber varies as a function of radial distance from the center of the fiber. In a step-index fiber, the refractive index exhibits an abrupt change in value at the core/cladding boundary. In a graded-index fiber, the refractive index tapers off parabolically as the radial distance from the center of the fiber increases.

In a multimode fiber, many modes from the incident light ray propagate down the fiber. The actual number of modes depends on the core diameter, the numerical aperture and the wavelength. Because many modes propagate down the fiber, multimode fiber suffers from intermodal dispersion (discussed in Section 2.3.2), which greatly limits its bandwidth. Typical core diameters for multimode fiber are 50 $\mu$m.

In single-mode fibers, the core is so small that only the fundamental mode of the incident light ray is allowed to propagate. Because only one mode propagates, single-mode fiber is not hampered by intermodal dispersion. Single-mode fiber does, however, suffer from chromatic dispersion (discussed in Section 2.3.1), but its effects are not as great as those from intermodal dispersion in multimode fibers. Single-mode fibers have much higher bandwidths than their multimode counterpart.

Attenuation in optical fibers varies depending on the wavelength. Figure 2.1 (Sterling 1987) shows that minimum attenuation windows occur at the 850 nm, 1300 nm, and 1550 nm wavelengths. The 1550 nm wavelength is considered the wavelength of minimum attenuation.

Dispersion-shifted fibers are currently used in optical systems to take advantage of the minimum attenuation at the 1550 nm wavelength and the zero-dispersion at the 1300 nm wavelength. In a dispersion-shifted fiber, the core-cladding refractive-index profile is graded so that the zero dispersion wavelength, usually 1300 nm (discussed in Section 2.3.1.1), is shifted to 1550 nm. The obvious benefit is a fiber with a high bandwidth and minimal attenuation losses.

The choice for a receiver centers around the type of photodiode used. The photodetectors most commonly used in fiber optic systems are silicon positive-intrinsic-negative (PIN) photodiodes, and avalanche photodiodes (APD). The APD type cost five to ten times more than the PIN type, but they offer higher sensitivity (10 to 20 dB). In addition, APDs have a higher bandwidth. The disadvantage of APDs is that they require high voltage (hundreds of volts) compared to PINs (tens of volts) and have greater noise. APDs are also very susceptible to temperature changes.

The remainder of the system components can be selected noting the attenuation with respect to the wavelength. The attenuation values are used in the link power budget calculations.

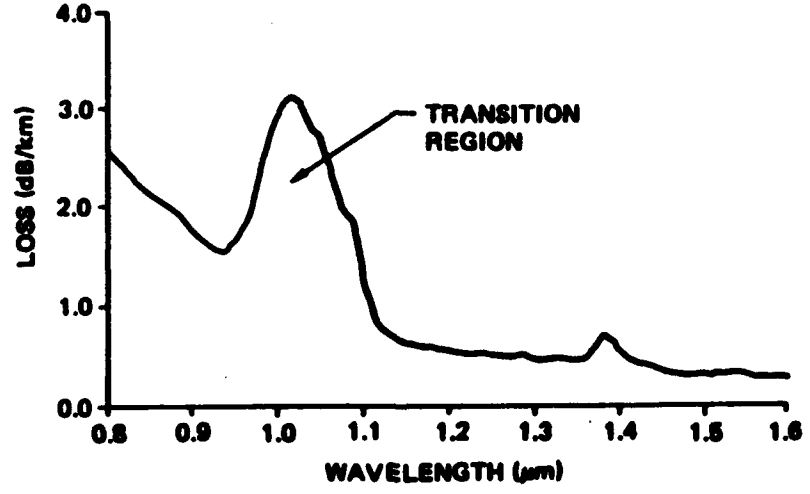


Figure 2.1 ATTENUATION vs. WAVELENGTH FOR SINGLE-MODE FIBER

The link power budget is derived from the sequential loss contributions of each element in the link. Each of these loss elements are expressed in decibels (dB). To satisfy the link power budget, the power budget between the transmitter power and the receiver sensitivity must be greater than the combined losses in the system.

## 2.2 Rise Time Budget

The rise time budget is a method for determining the dispersion limitation of the optical fiber link. In this calculation, the total rise time of the link is calculated from the root-sum-square of the rise times from the contributors in the link.

The basic elements that may significantly limit system speed are the transmitter rise time, the receiver rise time, and the dispersion in the system.

Since dispersion also limits the bandwidth of the system, the rise time budget analysis contributes to the calculation of the bandwidth limitations of the system. Because dispersion is such a limiting factor in the design of an optical link, its effects on system parameters and components are discussed further.

## 2.3 Dispersion

Dispersion is defined as the spreading of light pulses as they travel down the optical fiber. The pulse rate must be low enough so that the pulses do not overlap, resulting in loss of data. The lower the pulse rate (bandwidth), the greater the distance between adjacent pulses and, therefore, the greater the dispersion effect that can be

tolerated. The distortion (spreading) of the pulse is a consequence of intramodal dispersion and intermodal delay effects.

### 2.3.1 Intramodal Dispersion

Intramodal dispersion is defined as the pulse spreading that occurs within one of the guided modes traveling in the fiber and is a result of the group velocities' dependence on the wavelength $\lambda$. This type of dispersion is often referred to as chromatic dispersion. Because intramodal dispersion depends on the wavelength, its effect on signal distortion increases with the spectral width of the optical source. The spectral width is the band of wavelengths over which the source emits light and is normally characterized by the root-mean-square spectral width $\sigma_\lambda$ (Keiser 1983). Light-emitting diodes have a root-mean-square spectral width approximately five percent of the central wavelength, while laser diode optical sources have typical spectral width values of about 1 to 2 nm. Intramodal is generally caused by material and waveguide dispersions.

#### 2.3.1.1 Material Dispersion

Material dispersion arises from the variation of the refractive index of the core material as a function of wavelength as seen from the following equation

$$n = \frac{c}{v} \qquad (2.1)$$

where $n$ = refractive index

$c$ = speed of light

$v$ = speed of the particular mode travelling in the fiber

Each wavelength travels at a different speed through a material, so the value of v changes according to the wavelength. The amount of dispersion depends on two factors:

1. The spectral width of the optical source, which is basically the number of different wavelengths injected into the fiber.
2. The center operating wavelength of the source. Around 850 nm, longer wavelengths travel faster through an optical fiber than do shorter ones. The situation reverses at 1550 nm (the wavelength of minimum attenuation), as shorter wavelengths travel faster than longer ones. The crossover point, where shorter wavelengths begin to travel faster than longer ones, occurs around 1300 nm, sometimes called the zero-dispersion wavelength.

Figure 2.2 (Killen 1991) is a graph showing material dispersion for a typical single-mode fiber. At wavelengths below 1300 nm, dispersion is negative, so shorter wavelengths trail or arrive later at the fiber end. Above 1300 nm, shorter wavelengths lead or arrive faster at the fiber end. Material dispersion is, therefore, of particular importance for single-mode fibers and for the broader output spectrum LED systems.

To calculate material dispersion, a plane wave propagating in an infinitely extended dielectric medium with refractive index $n(\lambda)$ is considered. As the signal propagates along the fiber, each spectral component travels independently and undergoes a time delay or group delay per unit length given by Keiser (1983), Miller et al. (1973, pp. 1703-1751), and Dyott et al. (1971, pp. 82-84).

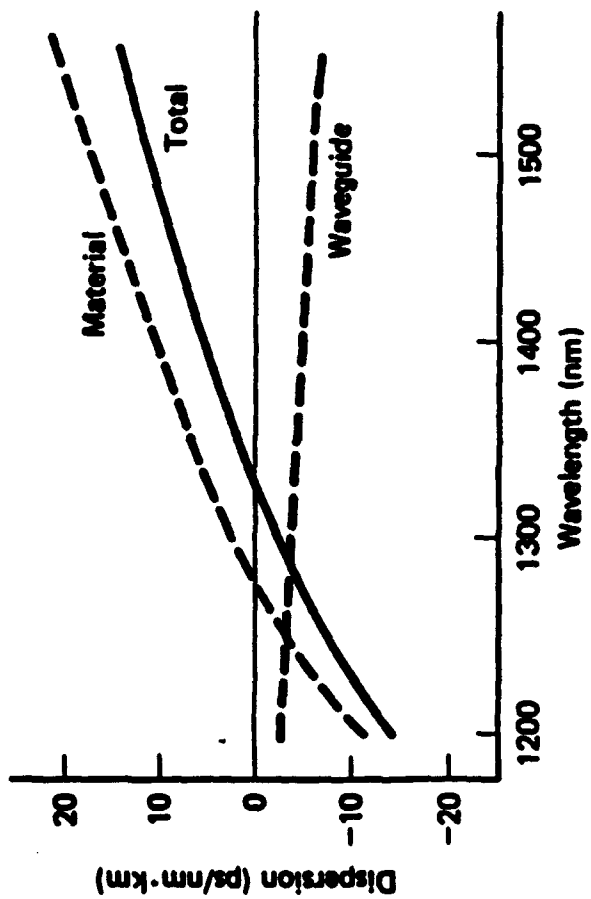


Figure 2.2 FIBER DISPERSION CHARACTERISTICS

$$\frac{t_{mat}}{L} = \frac{1}{V_g} = \frac{1}{c} d\beta/dk \qquad (2.2)$$

where $L$ = distance traveled by the pulse

$k = 2\pi/\lambda$

$\beta$ = propagation constant along the fiber = $\frac{2\pi n(\lambda)}{\lambda}$

$V_g$ = group velocity = $c(d\beta/dk)^{-1}$

Substituting $\beta$ and $k$ into equation (2.1) yields the group delay $t_{mat}$ resulting from material dispersion.

$$t_{mat} = \frac{1}{c}\left(n - \lambda \frac{dn}{d\lambda}\right) \qquad (2.3)$$

If the spectral width of the optical source is not too wide, the delay difference per unit wavelength along the propagation path is $\frac{dt_{mat}}{d\lambda}$. For special components which are $\Delta\lambda$ apart and lie $\frac{\Delta\lambda}{2}$ above and below a central wavelength, the total delay difference $\tau$ over a distance L is

$$\tau_{mat} = \frac{dt_{mat}}{d\lambda} \Delta\lambda \qquad (2.4)$$

If the spectral width $\Delta\lambda$ of an optical source is characterized by its root-mean-square value $\tau_\lambda$, the pulse spreading from material dispersion becomes

$$\tau_{mat} = \frac{dt_{mat}}{d\lambda} \sigma_\lambda = -\frac{L}{c} \lambda \frac{d^2n}{d\lambda_2} \sigma_\lambda \qquad (2.5)$$

The factor $D_{mat}$, designated as the material dispersion, is

$$D_{mat} = -\frac{1}{L}\frac{dt_{mat}}{d\lambda} = \frac{\lambda}{c}\frac{d^2n}{d\lambda^2} \qquad (2.6)$$

from the IEEE definition in IEEE Standard 812 (1984).

Substituting equation (2.6) in (2.5) yields

$$\tau_{mat} = D_{mat} \cdot \Delta\lambda \cdot L \qquad (2.7)$$

which is the group delay with respect to wavelength from the effects of material dispersion. The effects of material dispersion can be reduced by selecting sources with narrower spectral output widths or by operating at longer wavelengths.

2.3.1.2 Waveguide Dispersion

Waveguide dispersion is most significant in a single-mode fiber because the optical energy travels in both the core and cladding, which have slightly differing refractive indices. This type of dispersion is a result of the wavelength-dependence of the modal characteristics of the fiber because the geometry of the fiber causes the propagation constant of each mode to change if the wavelength changes.

In multimode fibers, the effects of waveguide dispersion can be neglected because it is very small compared to the effects of material dispersion. For single-mode fibers, waveguide dispersion can be on the same order of magnitude as material dispersion and must be considered.

The group delay caused by waveguide dispersion from Keiser (1983) and Killen (1991) is

$$t_{wg} = \frac{L}{c}\frac{d\beta}{dk} = \frac{L}{c}\left[n_2 + n_2\Delta\frac{dkb}{dk}\right] \tag{2.8}$$

where $\beta = n_2k(b\Delta + 1)$

$$\Delta = \frac{(n_1 - n_2)}{n_1}$$

The modal propagation constant $\beta$ can be given in terms of the normalized frequency $v$ from Keiser (1983) as

$$\nu = kan_2\sqrt{2\Delta} \tag{2.9}$$

and equation (2.8) becomes

$$t_{wg} = \frac{L}{c}\left[n_2 + n_2\Delta\frac{d(\nu b)}{d\nu}\right] \tag{2.10}$$

Using the same techniques as for material dispersion, the group delay with respect to wavelength for waveguide dispersion becomes

$$\tau_{wg} = \tau_\lambda\frac{dt_{wg}}{d\lambda} = -\frac{n_2L\Delta\tau_\lambda}{c\lambda}\,\nu\frac{d^2(\nu b)}{d\nu^2} \tag{2.11}$$

Substituting the waveguide dispersion factor $D_{wg}$

$$D_{wg} = -\left[\frac{\nu n_2\Delta}{\lambda c}\right]\frac{d^2(\nu b)}{d\nu^2}$$

into equation (2.11) yields

$$\tau_{wg} = D_{wg}\Delta\lambda L \qquad (2.12)$$

Figure 2.2 shows values of $D_{mat}$ and $D_{wg}$ with respect to wavelength.

Since both material and waveguide dispersions are summed to get chromatic dispersion, the factor $D_{chromatic}$ is defined as

$$D_{chromatic} = D_{mat} + D_{wg} \qquad (2.13)$$

2.3.2 Intermodal Dispersion

The second factor causing signal distortion in optical fibers is intermodal dispersion. This type of dispersion arises from the different values of the group delay for individual modes and results in the different modes arriving at the end of the fiber at different times. Because only one mode propagates in a single-mode fiber, intermodal dispersion is neglected.

For multimode fibers, the pulse broadening from intermodal dispersion is the difference in travel time between the longest ray congruence paths (highest-order mode) and the shortest ray congruence paths (fundamental mode) (Keiser 1983). The result is obtained from ray tracing and is given by

$$\tau_{mod} = T_{max} - T_{min} = \frac{n_1\Delta L}{c} \qquad (2.14)$$

Both intramodal and intermodal dispersion effects limit the bandwidth of the optical fiber.

## 2.4 Fiber Bandwidth

Fiber bandwidth is characterized in the time domain as dispersion. The effects of dispersion causes a pulse to broaden as it travels down the fiber. This pulse broadening will eventually cause neighboring pulses to overlap to the point where adjacent pulses can no longer be individually distinguished. As such, the dispersive properties determine the limit of the information capacity of the fiber.

A measure of the information capacity of an optical fiber is specified by the bandwidth-length product. To calculate this parameter, the optical power emerging from the fiber is assumed to have a Gaussian temporal response described by Hewlett Packard Co. (1989) and Keiser (1983).

$$g(t) = \frac{1}{\sqrt{2\pi}\sigma} e^{-t^2/2\sigma^2} \qquad (2.15)$$

where $\sigma$ is the rms pulse width.

The Fourier transform of this function is

$$G(\omega) = \frac{1}{\sqrt{2\pi}} e^{-\omega^2\sigma^2/2} \qquad (2.16)$$

In the field of optical fibers, bandwidth is characterized by $B_{3dB}$, the 3 dB optical corner frequency, and is defined as the modulation frequency at which the received optical power has fallen to 1/2 of the zero frequency value. Thus, from equation (2.15), the time $t_{1/2}$ required for the pulse to reach its half-maximum value occurs when

$$g(t_{1/2}) = 0.5\, g(0) \tag{2.17}$$

and is given by

$$t_{1/2} = (2\ln 2)^{1/2}\,\sigma \tag{2.18}$$

Then the full width of the half-maximum value can be defined as

$$t_{FWHM} = 2t_{1/2} = 2\sigma(2\ln 2)^{1/2} \tag{2.19}$$

Thus from equations (2.16) and (2.19), the relation between $t_{FWHM}$ and $B_{3dB}$, assuming a Gaussian response, is

$$B_{3dB} = \frac{0.44}{t_{FWHM}} \tag{2.20}$$

The cause of the finite width of the response can be represented by the quadratic addition of the intermodal and intramodal dispersion of the fiber (Hewlett Packard Co. 1989).

$$t_{FWHM} = \sqrt{\left(\frac{Ln_1}{c}\Delta\right)^2 + (L\Delta\lambda D_{chromatic})^2} \tag{2.21}$$

The fiber bandwidth length product is found by substituting equation (2.21) into equation (2.20) to become

$$B_{fib} \cdot L = \frac{0.44}{\sqrt{\left(\frac{n_1}{c}\Delta\right)^2 + (\Delta\lambda D_{chromatic})^2}} \tag{2.22}$$

## 2.5 Bit Error Rate

The bit error rate (BER) is defined as the number of erroneous bits received at the receiver divided by the total number of received bits. A ratio of $10^{-9}$ means that one wrong bit is received for every 1 billion bits transmitted. The BER varies with each application. Digitally encoded telephone voices have a higher BER requirement than digital computer data because a few faulty bits does not cause noticeable distortion in a voice but can cause considerable errors in computer data.

Dispersion effects for the optical system must be fully considered as adjacent pulses could overlap, resulting in a much higher BER than planned. The type of data-encoding format also affects the BER.

A widely used data-encoding format used for optical links is Manchester encoding. A Manchester code uses a level transition in the middle of each bit period. This code is obtained from a direct modulo-2 addition of the serial data and its clock. The result is a single return-to-zero (RZ) bitstream that contains both the data and its synchronized clock. At the fiber end, the Manchester code can be decoded such that the data and clock are extracted from the bitstream and are returned to their respective input states. The Manchester code helps eliminate DC and low-frequency noise and prevents possible receiver saturation during the transfer of many logical 1's in the case of non-return-to-zero (NRZ) data.

The dominant noise source in an optical system is usually the receiver. The receiver for the system must be selected such that its sensitivity is the minimum optical

power amplitude in order to achieve the required BER. Based on the assumption of a Gaussian distribution of noise amplitudes, an optical signal-to-noise ratio (SNR) of about 10 $dB_{opt}$ is required to obtain a BER of $10^{-9}$. An empirical formula for the sensitivity attainable with PIN type detectors is

$$S = -33 + 14 \log B \qquad (2.23)$$

where S = receiver sensitivity

B = bit rate in Gbit/s

Given the discussed limiting factors in the design of an optical system, the results derived are used to complete the design of the fiber optic data link.

# Chapter 3

## SYSTEM REQUIREMENTS

To sufficiently test and verify undersea concepts, autonomous underwater test vehicles are used. These vehicles can transmit and receive acoustic signals, process the received signal to obtain various types of acoustic information, and record both the raw acoustic data and the processed data. During a typical field test, the submerged test vehicle is launched from a surface craft to perform basic maneuvers to obtain acoustic information. When an acoustic source is detected, the vehicle attempts to identify the source's origin. The recorded data from the experiment is later analyzed to determine the correctness of the decision-making process of the data processors.

The technology of the vehicle must be kept current to test and verify new concepts. This requires higher data rates and increased data processing capabilities. The physical constraints of the vehicle limit the equipment used for an experiment. Moving the data processing and recording functions to the launch craft to take advantage of the available space alleviates this limitation. A fiber optic link was proposed to provide the data path between the vehicle and its launch craft.

The fiber optic link was designed into an underwater test vehicle using mainly self-contained, commercially available components. Major components of this link include the electronics necessary to interface the optical components to the existing hardware, a fiber optic transmitter/receiver (tx/rx) pair for each direction of transmission, the optical fiber, built into a micro-cable for strength, a bulkhead penetrator between the wet

(fiber) and dry (electronics) sections of the vehicle, wavelength division multiplexers (WDMs), and connectors.

The ultimate goal of the design is an operational bidirectional data link between the launch craft and the underwater vehicle. The link must be transparent to the vehicle, the launch craft, and their respective on-board components. The link should not hinder the vehicle as it travels through the water or prevent data flow from the sonar electronics to the data processor and recorder. To accomplish this, the following design requirements were followed:

- Commercially available stand-alone packages must be used to minimize mechanical modifications (also minimizes component design effort).
- Dispersion-shifted, single-mode fiber is used.
- The link should operate at distances up to 20 km, the maximum fiber spool size available from the manufacturer.
- The interface electronics must function in existing chassis and backplanes.
- The link should be designed using a BER of $10^{-9}$.
- Any required electrical power must be derived from the ±15 VDC, ±5 VDC, or ±28 VDC supplies in the vehicle.
- Data rates up to 32 MHz must be achievable. The current data rate is 16 MHz for non-return-to-zero (NRZ) format and 32 MHz if return-to-zero (RZ) coding is used.
- Design objectives must be satisfied, and future upgrades, including longer distances or increased data rates, must be accommodated.

Chapter 4 provides detailed descriptions of the design process for the link, including the selection of the optical components, calculations to verify operation of link on paper, and the design of the interface electronics. Chapter 5 describes the testing conducted to verify operation of the link, and Chapter 6 provides a discussion of the test results.

# Chapter 4

# SYSTEM DESIGN

## 4.1 Overview of the System

A block diagram of the underwater vehicle showing the major components, including the fiber optic link, is shown in Figure 4.1.

The underwater portion of the vehicle consists of a sonar section, a signal conditioning and A/D assembly, a data processor, a data recorder, and the components of the fiber optic link. The sonar section transmits and receives acoustic signals to/from the surrounding water. The received analog signals are input to the signal conditioners where they are filtered for unwanted noise and amplified. These amplified signals are digitized in the A/D assembly and sent to the vehicle-based fiber optic link. The link is responsible for routing the digitized sonar data to the on-board data processor and data recorder and for transmitting the data up the link to the launch craft.

The launch-craft-based fiber optic link receives the optical data from the vehicle, converts it to an electrical format, and inputs the data to an on-board data processor and recorder. The link also transmits steering commands and directional data from the data processor to the vehicle based on the received sonar data. The launch craft and the underwater vehicle are spanned by a fiber optic cable of lengths up to 20 km. The fiber optic link and interface electronics are designed to be transparent to the other system components.

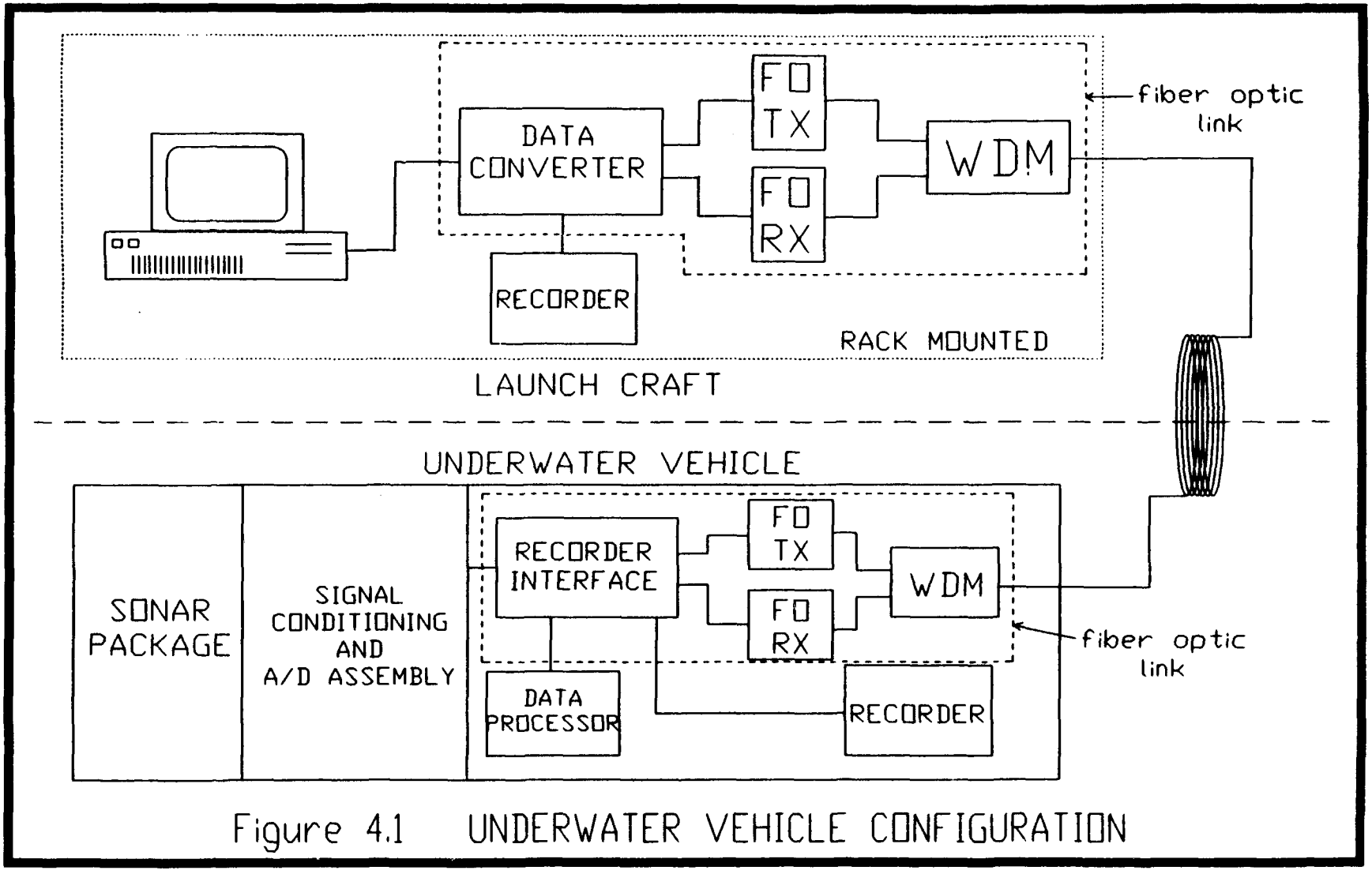


Figure 4.1 UNDERWATER VEHICLE CONFIGURATION

## 4.2 Design and Selection of Link Components

As discussed Chapter 2, the design of an optical link involves the interrelationship of its components, of which the fiber, the transmitter, and the receiver are most important. The components for the link must be carefully selected to ensure the following key requirements are achieved:

- transmission distance -- up to 20 km
- data rate -- initially 16 Mbits per second NRZ
- bit error rate (BER) -- $10^{-9}$

The optical components and the choices (if any) considered for each component to satisfy the requirements are:

- transmitter -- LED or laser diode
- receiver -- PIN- or APD-type photodiode
- wavelength division multiplexers -- angular dispersive or filter based
- connectors -- SMA-type, ST-type, or Biconic
- penetrator
- fiber optic cable -- single-mode

Before any components are selected, a guideline link power budget is calculated. This calculation, described in Section 4.2.1, uses average values for the components in the system. The results of this calculation establish a range of operating characteristics for all link components, thus simplifying the selection process. Only components operating in the calculated range are considered.

In Sections 4.3 through 4.7, the optical components are described in detail. The different choices for each component are contrasted, followed by an explanation of why the particular component was chosen. Also, both the optical and electrical (where necessary) characteristics of the selected components are listed.

After selecting all link components, their respective characteristics are used in the link power budget and the rise time budget calculations to verify, at least on paper, proper link operation according to the objectives set in Chapter 1. These calculations are presented in Sections 4.8 and 4.9.

Finally, the design of the electronics required to interface the fiber optic link to the electronics in the underwater vehicle and launch craft is described in Sections 4.10 and 4.11.

### 4.2.1 Link Power Budget

The design of the fiber optic link involves many interrelated variables of the operating characteristics from the different components. As such, the actual link design sometimes requires several iterations before a design is reached that satisfies the operating parameters of the system. Also, performance and packaging are very important factors to be considered for the underwater vehicle. The components chosen must function almost flawlessly to assure a successful test and must also be selected to minimize mechanical changes in the vehicle.

The link power budget analysis determines the achievable transmission distance given the components required for the fiber optic link. If the first link budget analysis does not provide for the distance required, components must be changed. Since the fiber optic link is a new design without any previous information for referral, a very basic link budget is calculated to determine base requirements in the actual selection of components.

To begin link power budget calculations, the wavelengths required for bidirectional communication must be decided. The desired transmission distance for this link ranges up to 20 km, which is considered to be a relatively long distance. As such, wavelengths offering low attenuation were considered. From Figure 2.1, two low loss wavelengths selected are 1300 nm and 1550 nm.

The 1300 nm wavelength was selected for the low data rate transmission from the launch craft to the vehicle, and the 1550 nm wavelength was selected for the high data rate transmission from the vehicle to the launch craft. The 1300 nm wavelength is considered relatively low loss and offers zero dispersion. The 1550 nm wavelength has minimal loss, but does suffer from the effects of chromatic dispersion. Dispersion characteristics are shown in Figure 2.2.

The 1550 nm wavelength was chosen for the higher data rate uplink for the following reason. From Chapter 2, the receiver sensitivity level is approximately proportional to the square root of its bandwidth; so, the sensitivity of the low data rate receiver (1300 nm) is much better than that of the high data rate receiver (1550 nm).

The 1550 nm wavelength, however, has lower attenuation characteristics than the 1300 nm wavelength. As such, the additional fiber losses at 1300 nm are compensated by the higher sensitivity of its receiver (Brininstool 1987).

After the wavelengths of operation are defined, the optical components of the link are chosen. The average loss values of these components are used in the initial power budget calculation to determine operating ranges to aid in component selection. The following is a brief description of the components and their average loss characteristics. Detailed descriptions of the components and choices are provided in Sections 4.3 through 4.7.

- Optical Fiber -- Dispersion-shifted single-mode fiber is used. Typical attenuation values for this type of fiber is 0.5 dB/km.
- Wavelength Division Multiplexer (WDM) -- A complementary 1300 nm/ 1550 nm WDM pair is required (a 1300 nm MUX/1550 nm DEMUX and a 1550 nm MUX/1300 nm DEMUX). Attenuation is approximately 4 dB, including connectors.
- Transmitter/Receiver (tx/rx) Pair -- The tx/rx pair must be chosen so their power margin (tx power out - rx sensitivity) is greater than the losses for the system. The choices for the transmitter are laser and LED types; the choices for the receiver are PIN and APD types.

| tx output power | |
|---|---|
| LED | -23 dBm |
| Laser | 0 dBm |
| **rx sensitivity** | |
| PIN | -35 dBm |
| APD | -43 dBm |

- Penetrator -- The penetrator mounts into the bulkhead to provide physical separation between the vehicle electronics (dry section) and the fiber payout spool (wet section). Attenuation is approximately 2 dB for insertion loss.
- Connectors -- Single-mode type connectors are required. The connector type must be consistent throughout the system. Typical losses are 0.5 dB for single-mode connectors.

Figure 2.3 is used as the model for the following power budget calculations. The analysis is completed assuming a worst-case link distance of 20 km. The link loss budget is derived from the sequential loss contributions of each component in the link. The loss of these components is expressed in decibels (dB) and is calculated by:

$$\text{Loss} = 10\log(\text{Pout}/\text{Pin}) \qquad (4.1)$$

where Pin and Pout are the optical powers into and out of the component. The optical power received at the receiver is dependent on the amount of light coupled into the fiber and the losses incurred in the fiber and in the link.

Not shown in Figure 4.2 is a safety margin to account for component aging, temperature fluctuations, and losses for components that might be added in the future.

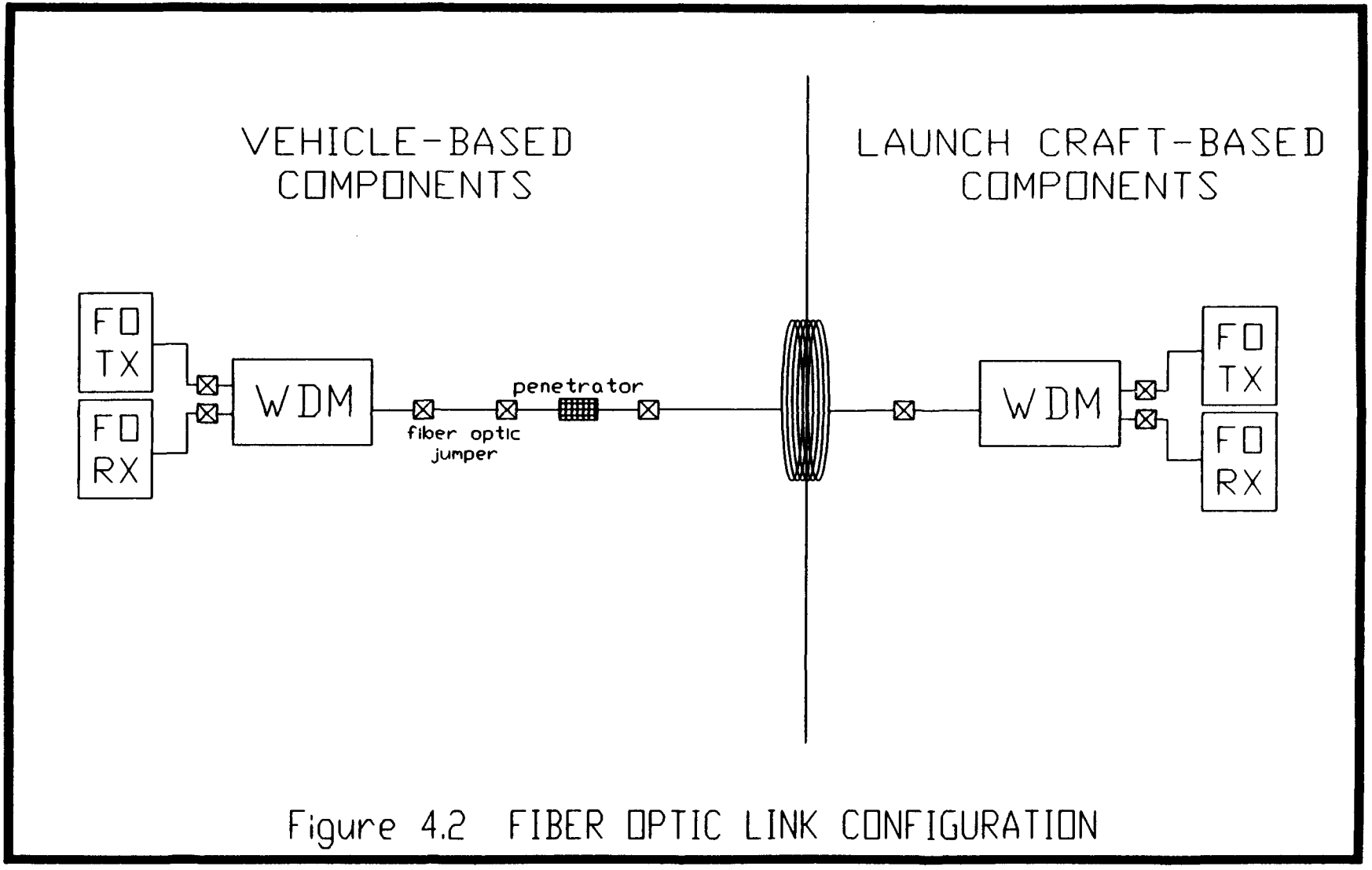


Figure 4.2 FIBER OPTIC LINK CONFIGURATION

Typical safety margins range from a minimum of 3 dB to a conservative 10 dB. An estimate of 10 dB is used as a safety margin for the vehicle.

Given the above information, a preliminary power/loss equation is written for Figure 4.2.

$$P_{tx} - P_{rx} \geq P_{sys} + P_{saf} \tag{4.2}$$

where $P_{tx}$ = power out of transmitter

$P_{rx}$ = sensitivity of receiver

$P_{saf}$ = safety margin = 10 dB

The system component losses ($P_{sys}$) for the link are as follows:

$$P_{sys} = 2P_{wdm} + 8P_{con} + 2P_{jmp} + P_{pen} + 20 * (P_{cab}) \tag{4.3}$$

where $P_{wdm}$ = the loss associated with the WDM = 4 dB

$P_{con}$ = loss per connection = 1 dB

$P_{jmp}$ = loss of fiber jumper internal to vehicle = 1.5 dB

$P_{pen}$ = loss of penetrator = 2 dB

$P_{cab}$ = loss of cable = 0.5 dB/km

Using the above losses, the system loss for a 20 km distance is calculated to be

$$P_{sys} = 2*(4\,dB)+8*(1\,dB)+2*(1.5\,dB)+2\,dB+20\,km*(0.5\,dB/km) \tag{4.4}$$

$$P_{sys} = 31\,dB$$

When the safety margin, $P_{saf}$, is included, equation (4.2) becomes

$$P_{tx} - P_{rx} \geq 31\,dB + 10\,dB = 41\,dB. \qquad (4.5)$$

The flux budget of the transmitter/receiver pair must be greater than or equal to 41 dB. The loss characteristics used in the analysis are not "hard" numbers. Some components might have better characteristics, some worse, and what might be gained with one component might be lost with another. The link components are selected using the typical values provided in this section.

## 4.3 Transmitter/Receiver Selection

Commercial transmitter/receiver components are used because they offer stand-alone packaging and require no external components. A matched transmitter/receiver pair was selected rather than components from different vendors. Matched components offer the advantage of a tested, stand-alone system, and the receiver output data format is the same as the format input to the transmitter. Also, more technical support is available if a problem occurs.

The four requirements for the pair are:

- no external components
- support of single-mode fiber
- operation at data rates of up to 16 Mbps NRZ for initial system
- an approximate flux budget of 41 dB

There are two basic choices for the type of transmitter to use -- an LED transmitter or a laser diode transmitter.

LED transmitters are designed around either a surface emitting or an edge emitting light emitting diode. The LEDs emit light spontaneously when a forward bias is applied across the device. The resulting light is a low radiance output whose large pattern is not suited for use with small optical fibers because only a small portion of the light is coupled into the fiber. LEDs operate in the 800 to 1300 nm window (Botez 1979, pp. 1230-1238).

Laser diodes, on the other hand, provide stimulated emission of light rather than spontaneous emission (Sterling 1987). The laser acts like an LED at low currents, but as the current increases, lasing action begins. The laser relies on a high current density to provide the lasing action. The lasing occurs when some of the photons are trapped in the Fabry-Perot cavity, reflecting from end mirror to end mirror. In a distributed-feedback (DFB) laser, the lasing action is obtained from Bragg reflectors or periodic variation (gratings). In either type, these trapped photons stimulate the emission of other photons, which results in amplification. Light is produced when some of the photons escape through the two end faces. The light is then coupled into a fiber. The light emitted from the laser has a narrow band of wavelengths and is, therefore, nearly monochromatic (Keiser 1983).

For this long-distance application (up to 20 km), a laser diode type of transmitter was selected. A laser diode is preferred over an LED transmitter for the following

reasons: higher output power capability, narrow spatial emission pattern for efficient coupling to single-mode fibers, a narrow spectral linewidth which minimizes material dispersion, and rise times that are an order of magnitude faster than LEDs (Brininstool 1987). Also, LED sources operating at 1550 nm are not readily available.

The transmitter selected is a 500 Mbit/sec digital, DFB-type transmitter. This package accepts electrical information as input and outputs optical signals. Electrical data is converted into optical data by modulating an internal injection laser diode. Strapping options allow the transmitter to accept either TTL- or ECL-level signals. The ECL option supports data rates from DC to 500 Mbps (NRZ), and the TTL option supports data rates from DC to 50 Mbps (NRZ). Although the TTL option satisfies current data rate requirements, the ECL option is used for the link to allow for future upgrades in data rate.

Two laser diode transmitters are required for the system. One operates at 1300 nm and is used to transmit information from the launch craft to the underwater vehicle. The other transmitter, located in the vehicle, operates at 1550 nm and transmits data to the launch craft.

The choice of a matching receiver for the transmitter centers around the type of photodetector, either PIN or APD, used in the receiver. The PIN detector is the most widely used photodetector due to its simplicity, stability, and bandwidth. APDs have higher effective responsivities and are more sensitive; however, they are less stable over

temperature variations and often require a large bias voltage for operation, which is not readily available on the vehicle.

As such, the receiver for the link incorporates a PIN photodiode module with high sensitivity and a wide dynamic range. The receiver consists of a single-mode fiber pigtail coupled to an InGaAs PIN detector which drives a hybrid transimpedance preamplifier. Like the matching transmitter, the receiver interfaces to standard ECL electronics. Two receivers are used in the link. One is located in the vehicle and operates at 1300 nm, and the other is located on the launch craft and operates at 1550 nm.

The performance parameters for the transmitter/receiver pairs are given in Table 4.1 (Laser Diode Inc. 1990).

The connectors used on the fiber pigtails of the transmitter/receiver pairs are ST-type bayonet fiber optic connectors.

Table 4.1 Performance Parameters for the Transmitter/Receiver Pair

| **Transmitter/Receiver Model:** | LDDL-2510 | LDDL-2515 |
|---|---|---|
| **Transmitter** | | |
| Wavelength | 1300 nm | 1550 nm |
| Data rate (optimized) (up to 500 Mbps max) | 20 Mbps (RZ) | 20 Mbps (RZ) |
| Power out from pigtail (including connectors) | -3 dBm (avg.) | -5.6 dBm (avg.) |
| Rise/fall time | 1/1 ns (typ.) | 1/1 ns (typ.) |
| Spectral width | 5 nm | 5 nm |
| Supply voltage | pos. 5.0 VDC<br>neg. -5.2 volts | pos. 5.0 VDC<br>neg. -5.2 volts |
| Supply current | pos. 75 mA (max.)<br>neg. 500 mA (max.) | pos. 75 mA (max.)<br>neg. 500 mA (max.) |
| **Receiver** | | |
| Wavelength | 1300 nm | 1550 nm |
| Data rate (optimized) | 20 Mbps (RZ) | 20 Mbps (RZ) |
| Sensitivity (including connectors) | -46 dBm | -46 dBm |
| Dynamic range | >25 dB | >25 dB |
| Bandwidth (3 dB) | 250 MHz | 250 MHz |

## 4.4 Wavelength Division Multiplexing

To achieve simultaneous, bidirectional communication, a pair of complementary wavelength division multiplexers (WDM) are used. A WDM supports bidirectional data transmission by passing a particular wavelength in one direction, extracting the second wavelength from the other direction and routing it toward its target location, while isolating both wavelengths and their respective components from each other. For example, a 1300 nm WDM injects outgoing light from the 1300 nm transmitter into the optical fiber and extracts the distant 1550 nm transmitter signal, directing it to the 1550 nm receiver. Figure 4.3 shows the basic operation of the WDM pair (JDS Optics 1991).

There are three major design concerns to consider when using WDMs: insertion loss, cross talk, and isolation (Ito et al. 1981, pp. 84-86; Sugimoto et al. 1977, p. 680-682).

The ideal WDM has zero insertion loss, defined as the ratio of the power input to the connector at the input port to the power output from the respective output connector. The measured worst-case insertion loss for the WDM used for the vehicle is 0.7 dB, including the loss of the connectors.

Cross talk occurs when there is insufficient isolation between the two wavelengths such that they impinge on each other and cause errors in the data. In design practice, the optical leak-through of the local transmitter into the local receiver port should be limited to a level well below the operational noise floor of the receiver (Keiser 1983).

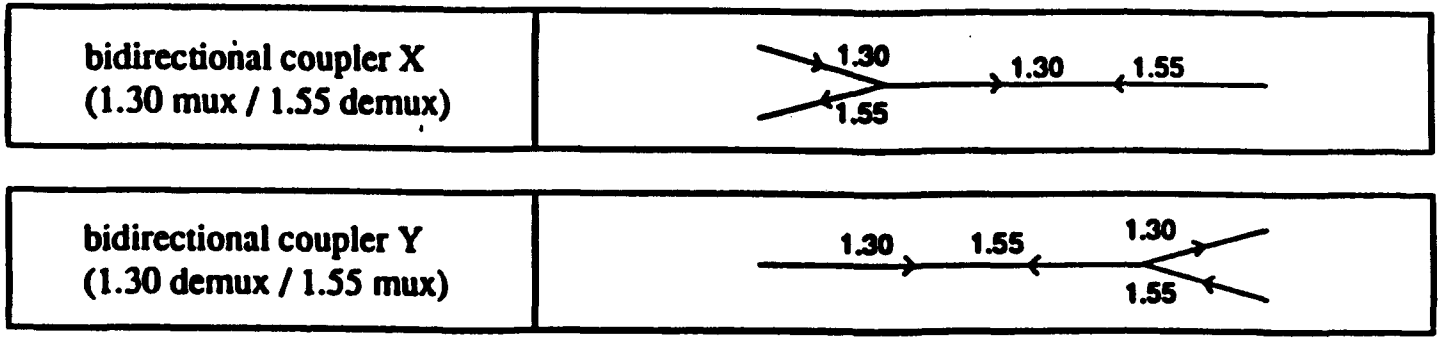


Figure 4.3 BASIC WDM OPERATION

The optical signal-to-noise ratio (SNR) is another method of determining the minimum allowable cross talk level at the local receiver. For a digital system to maintain a bit error rate (BER) of $10^{-9}$, the SNR must be about 10 dB minimum, from Chapter 2. Therefore, the local transmitter power level must be at least 11 dB lower at the receiver port than the received incoming signal power level to prevent interference (Brininstool 1987). The cross talk for the WDM is measured at less than -40 dB.

The ideal WDM also has infinite isolation. This isolation is defined as the attenuation of the local transmitter signal achieved relative to the local receiver port. As for cross talk, the WDM must provide enough isolation so that the signal from the local transmitter is attenuated to a level less than the minimum sensitivity of the local receiver. The measured isolation for the WDM in use is less than -60 dB.

The most widely used WDMs can be classified into two categories: angularly dispersive devices (such as prisms or gratings) and filter-based devices (such as multilayer thin-film interference filters). The WDMs in use for this design fall into the second category. The basic operation of a filter-based device is shown in Figure 4.4 (Keiser 1983).

The filters are designed to pass light of a specific wavelength and reflect all other wavelengths. The reflective filters are designed utilizing a glass substrate upon which as many as 16 separate optical layers are deposited for wavelength sensitivity (JDS Optics 1991). For systems including more than two wavelengths, these filters can be placed in series to separate the additional wavelengths. Due to design complexity and increase in

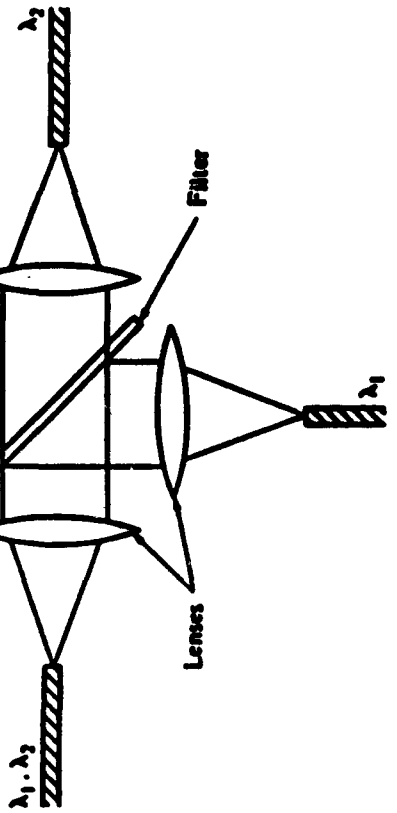


Figure 4.4 WDM USING THIN-FILM FILTER

passband signal loss, the number of filters are generally limited to two or three (Keiser 1983).

The manufacturer's specifications for the WDMs delivered for this design and the measured values are shown in Table 4.2 (JDS Optics 1991). The actual loss values were much less than the 4 dB values used in the initial power loss budget calculations.

## 4.5 Connectors

The most important parameter concerning optical connectors is loss from insertion and reflection. Because of the small core diameter of single-mode fibers (typically 9 $\mu$m), mechanical alignment of the fibers and their respective connectors are critical.

A connector should align the fibers on their center axes. When the center axes do not coincide, a loss occurs. As shown in Figure 4.5 (Sterling 1987), the amount of displacement depends on the ratio of the lateral offset to the fiber diameter; thus the acceptable offset is less as the fiber diameter gets smaller. This type of loss is considered insertion loss.

Reflection loss occurs when the two fibers are separated by a small gap, as shown in Figure 4.6 (Sterling 1987). Ideally, the fibers should butt to eliminate the gap. In most cases, however, a small gap is desirable to prevent abrasion or even fracturing on the fiber ends. Most connectors are designed to maintain a very small gap between the fibers.

Table 4.2 WDM Manufacturer's Specifications and Measured Values

Model 1315Y-A2 -- 1550 nm MUX/1300 nm DEMUX

| Parameter | Specification | Measured |
|---|---|---|
| MUX Channel Band | 1480 - 1600 nm | 1500 - 1580 nm |
| DEMUX Channel Band | 1250 - 1350 nm | 1275 - 1335 nm |
| Loss: | | |
| MUX Channel | 0.8 dB | 0.6 dB |
| DEMUX Channel | 0.8 dB | 0.7 dB |
| Cross Talk Isolation | < -30 dB | < -40 dB |
| Port Isolation | < -50 dB | < -60 dB |

Model 1315X-A2 -- 1300 nm MUX/1550 nm DEMUX

| Parameter | Specification | Measured |
|---|---|---|
| MUX Channel Band | 1250 - 1350 nm | 1270 - 1340 nm |
| DEMUX Channel Band | 1480 - 1600 nm | 1530 - 1600 nm |
| Loss: | | |
| MUX Channel | 0.8 dB | 0.3 dB |
| DEMUX Channel | 0.8 dB | 0.4 dB |
| Cross Talk Isolation | < -30 dB | < -40 dB |
| Part Isolation | < -50 dB | < -60 dB |

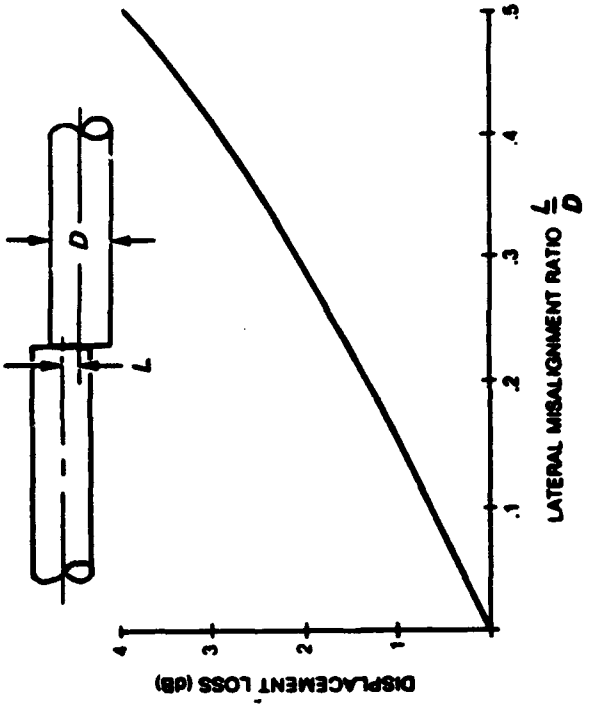


Figure 4.5 LOSS FROM LATERAL DISPLACEMENT

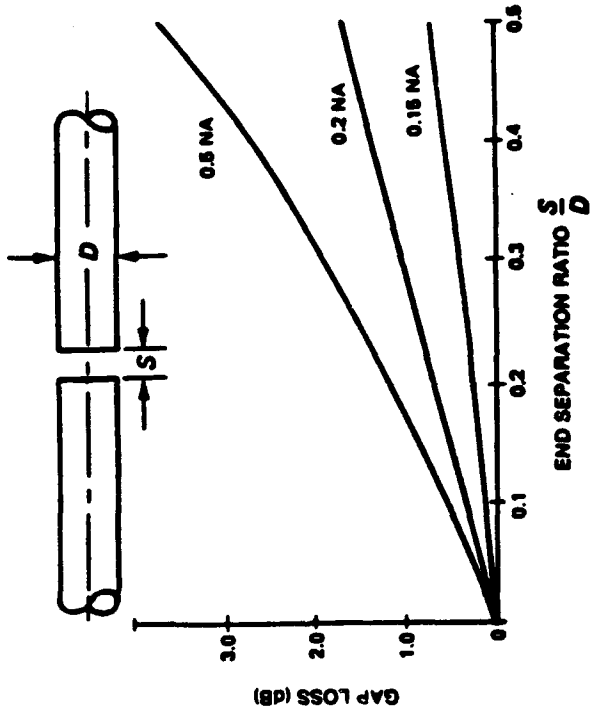


Figure 4.6 LOSS FROM END SEPARATION

The reflection loss, called Fresnel reflection loss, is caused by the differing reflected indices of the fiber and the small gap (Sterling 1987). When the incident light hits a new refractive index boundary, some of the light is reflected from the boundary in the opposite direction. Fresnel reflection occurs at both the exit of the first fiber from the fiber/air change in index and the entrance to the second fiber from the air/fiber index change boundary.

The most popular connectors are the SMA-type, ST-type, and biconic. These connectors are contrasted in Table 4.3 (OFTI 1987).

Table 4.3 Performance Parameters of Fiber Optic Connectors

| Parameter | SMA-type | ST-type | Biconic |
|---|---|---|---|
| Insertion Loss | 1 - 1.5 dB | 0.5 dB | 0.5 dB |
| Reflection | -20 dB | -30 dB | < -30 dB |
| Connection Type | threaded | bayonet | threaded |
| Durability (loss/500 connections) | ≤ 0.2 dB | ≤ 0.25 dB | ≤ 0.25 dB |

The ST-type connectors were selected for use in the fiber optic link for the vehicle. STs are considered the ultimate near-future replacement for most other connector technologies (Hewlett Packard Co. 1989). The ST design incorporates a bayonet-type coupling nut, similar to that of the BNC-type coaxial connector. The ST connector eliminates the fiber-to-fiber air gap, thus reducing Fresnel reflection, and

offers a keyed design, allowing each mating to be precisely positioned. The keyed design also prevents damage to the fiber caused by rotation while making fiber-to-fiber connections.

ST-type interconnections are made using an ST-type mating adaptor. The adaptor is constructed of nickel-plated zinc alloy and employs a split sleeve for the keyed design of the ST-type connector (OFTI 1987). The connectors plug into either end of the adaptor, and the fibers align and mate inside. The adaptors prevent angular misalignment, which occurs when the ends of the mated fibers are not perpendicular to the fiber axes during engagement.

The installed connectors in the link design have measured attenuations of less than 0.5 dB, consistent with the loss values used in the preliminary loss budget calculations.

## 4.6 Penetrator

An optical pressure penetrator is used to interface the low pressure environment of the vehicle electronics and the high pressure environment of the water. The penetrator mounts into the bulkhead that provides physical separation between the vehicle electronics and the canister that houses the fiber optic payout spool. The canister section is flooded with water to ease fiber payout. The bulkhead prevents water from entering the vehicle through the high-pressure canister section and interfering with the electronics. The penetrator is pressure-tested to exceed the depths encountered during the experiment.

The construction of the penetrator, shown in Figure 4.7, involves inserting a single-mode fiber into resilient, high-temperature thermoplastic sealants encased by a metal sheath. This assembly is packaged with a metal compression fitting. The result is a splice-free, uninterrupted fiber. ST-type fiber optic connectors are then installed at both ends.

The specifications for the penetrator used for the link design are:

- 9/125 micron dispersion-shifted single-mode fiber
- 6" fiber pigtails on both high and low pressure sides
- tested to 1000 psi operating pressure
- terminated with ST-type fiber optic connectors on both ends
- measured insertion loss of less than 1.5 dB
- 1/4" NPT mounting into bulkhead

The penetrator was custom made for this application by Conax Buffalo Corporation.

## 4.7 Fiber Optic Cable

Single-mode, dispersion-shifted fiber is used in the design. In a dispersion-shifted fiber, the zero-dispersion wavelength, usually 1300 nm, is shifted to 1550 nm (the wavelength of minimum attenuation) by grading the core-cladding refractive index profile (Brininstool 1987). The specifications of this commercial fiber, purchased from Corning Glassworks, are given in Table 4.4.

Because the fiber optic cable is static-mounted to the launch craft and payed out of the vehicle, a strength member was added to the fiber to provide additional tensile

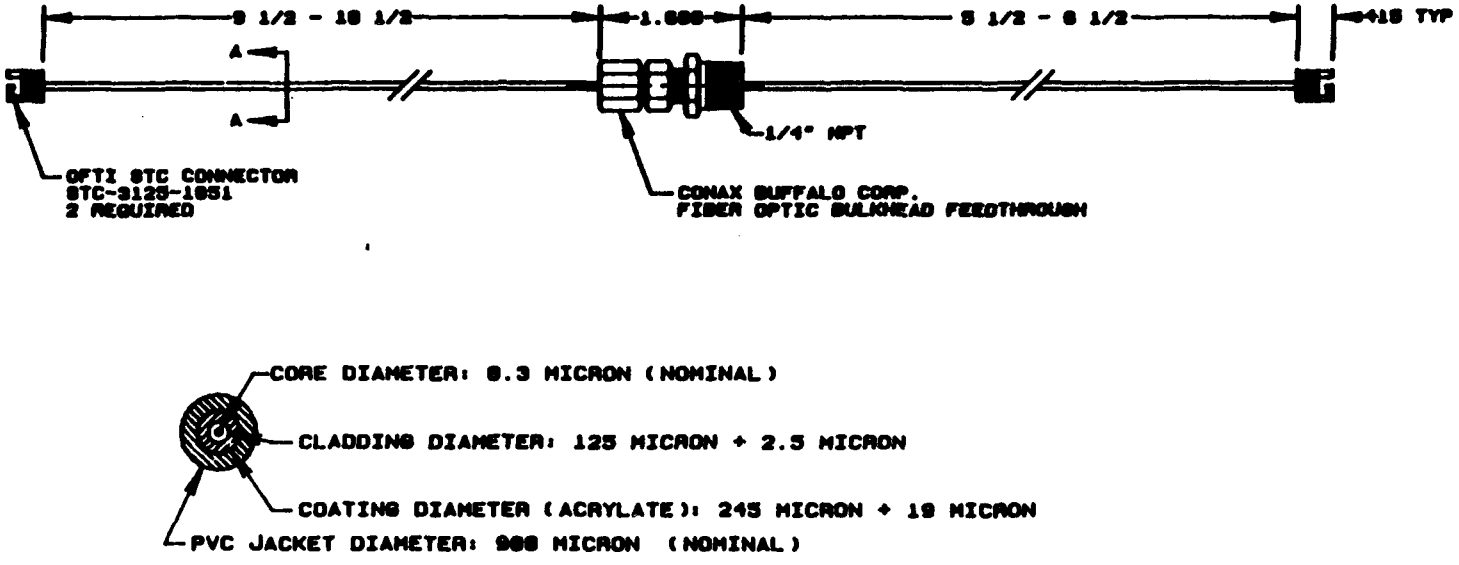


Figure 4.7 FIBER OPTIC PENETRATOR

Table 4.4 Specifications for the Optical Fiber

| **Optical Characteristics** | **Specified** | |
|---|---|---|
| Attenuation | 1550 nm<br>1300 nm | 0.25 dB/km<br>0.45 dB/km |
| Cutoff wavelength | | 1130 - 1270 nm |
| Dispersion | 1550 nm | 2.5 ps/nm-km |
| Mode field diameter | | 9 $\mu$m |
| Effective core refractive index | | 1.476 |
| **Physical Characteristics** | | |
| Cladding diameter | | 125 ±3 $\mu$m |
| CPC coating | | 250 ±15 $\mu$m |
| Proof test | | 0.35 GPa (50,000 psi) |

strength, stiffness, and ruggedness. The strength member consisted of the buffered optical fiber encased in fiber yarn to form a composite structure.

By adding the strength member, the tensile strength increases to a working force of 30 pounds. On the downside, the strength member increases the weight of the fiber to 44 pounds per 20 km, which consequently adds weight to the vehicle.

The strengthened cable is wound into free-standing coils and mounted inside the vehicle. The coils are wound such that when the vehicle is launched, the fiber pays out without twists or bends. A binding adhesive is used to keep the coil intact and to control the tension during fiber payout. A 20 km length of reinforced cable can be pre-twisted and wound into a cylindrical coil that is 7.63" high and has a 12.25" outer diameter and a 5.90" inner hole diameter.

Figure 4.8 shows an Optical Time Domain Reflectometer (OTDR) plot of a 9 km length of fiber, including the strength member, coiled for installation into the vehicle. The OTDR is a piece of optical test equipment used to plot the attenuation characteristics of the fiber continuously for the length of the fiber. The plot will identify cracks or breaks in the fiber and identify impurities or weaknesses in the glass.

It should also be noted that processing the fiber into a cable adds attenuation. Table 4.5 shows the step-by-step attenuation characteristics of the 20 km fiber from the initial fiber to adding the strength member to make the cable to coiling.

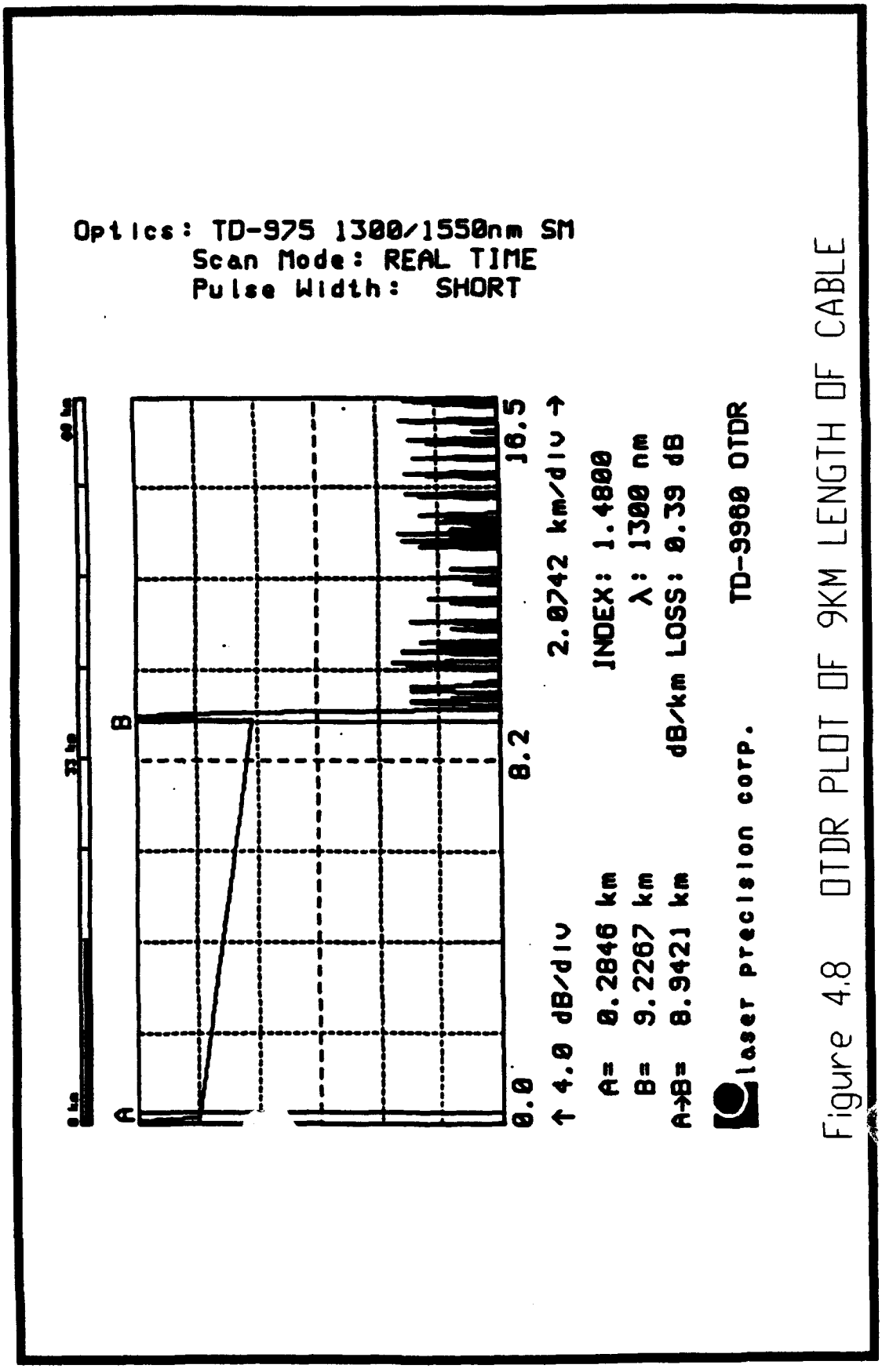


Figure 4.8 OTDR PLOT OF 9KM LENGTH OF CABLE

Table 4.5 Attenuation Characteristics

| Initial Fiber | After Cabling | Coiling |
|---|---|---|
| Length: 20081 meters | Length: 20000 meters | Length: 19573 meters |
| @ 1300 nm: 0.40 dB/km | @ 1300 nm: 0.42 dB/km | @ 1300 nm: 0.43 dB/km |
| @ 1550 nm: 0.22 dB/km | @ 1550 nm: 0.48 dB/km | @ 1550 nm: 0.53 dB/km |

## 4.8 Actual System Power Loss Budget

Using the optical characteristics of the chosen vehicle components, the actual power loss budget is calculated.

Table 4.6 summarizes the optical characteristics of the components described in Sections 4.3 through 4.7. A spare system was built in case problems developed in the first system, and the values used in Table 4.6 are the averages for each component type of both systems.

To calculate the actual power loss budget, the loss characteristics from Table 4.6 are plugged into equation (4.3). Worst-case numbers from the higher loss 1550 nm wavelength direction are used. Also, since loss parameters for all components except the fiber optic cable include connectors, the number of connectors considered in equation (4.3) drops from eight to two (one for either end of the spooled cable).

$$P_{sys} = 2P_{wdm} + 2P_{con} + 2_{jmp} + P_{pen} + P_{cab}$$
$$P_{sys} = 2*(0.6) + 2*(0.4) + 2*(1.1) + 1.3 + 20*(0.55) = 16.5\,dB \qquad (4.6)$$

Table 4.6 Power Loss Characteristics of Actual Link Components

| Component | | Characteristic |
|---|---|---|
| Transmitter | 1300 nm | -3 dBm |
| | 1550 nm | -5.6 dBm |
| Receiver | 1300 nm | -46 dBm |
| | 1550 nm | -46 dBm |
| WDM | 1300 MUX/1550 DEMUX | 0.4 dB/0.4 dB |
| | 1550 MUX/1300 DEMUX | 0.6 dB/0.6 dB |
| Connectors | | 0.4 dB |
| Penetrator | | 1.3 dB |
| Optical cable | 1300 nm | 0.43 dB/km |
| | 1550 nm | 0.55 dB/km |
| Optical jumper cable | | 1.1 dB |

Substituting the $P_{sys}$ value and the $P_{saf}$ = 10 dB value into equation (4.2), the flux budget required from the tx/rx pair is 26.5 dB. The calculated flux budget from Table 4.6 is -5.6 - (-46) = 40.4 dBm:

$$P_{tx} - P_{rx} \geq 16.5\,dB + 10\,dB = 26.5\,dB$$
$$P_{tx} - P_{rx} = 40.4\,dB > 26.5\,dB \qquad (4.7)$$

The flux budget of the tx/rx pair easily exceeds the required calculated value. By doing similar calculations for the 1300 nm direction, $P_{sys}$ is 13.7 dB, and the required flux budget is 23.7 dB, which is easily met. For link distances less than 20 km, the optical receiver becomes saturated because the power into the receiver exceeds its dynamic range. In these cases, attenuators are added.

The attenuators are called washer attenuators and they come in different thicknesses; the thicker the attenuator, the more attenuation. The attenuators are inserted over the ferrule of a connector and force an air gap between the fiber ends. The attenuators are color-coded, with each color designating a range of approximate attenuation values. Exact attenuation values cannot be given because they vary slightly with each application. An optical power meter should be used to measure these values.

## 4.9 Rise Time Analysis

With the components of the link selected and the power loss budget equation satisfied, a rise time analysis is conducted and the system bandwidth is calculated. The rise time analysis is a method for determining the dispersion limitations of the optical link.

The rise times of four basic link elements contribute significantly to limiting system speed. These elements are the optical transmitter, rise time $t_{tx}$, the material dispersion of the fiber, rise time $t_{mat}$, the modal dispersion of the fiber, rise time $t_{mod}$, and the optical receiver, rise time $t_{rx}$. All other factors which may lend to reducing system speed are negligible compared to these four limiting elements.

The system rise equation becomes the root-sum-square of the rise times of the limiting contributors:

$$t_{sys} = \sqrt{\sum_{i=1}^{n} t_i^2} \tag{4.8}$$

where $t_i$ is the rise times of the contributors.

When the four major contributors are substituted in, equation (4.8) becomes

$$t_{sys}^2 = t_{tx}^2 + t_{rx}^2 + t_{mod}^2 + t_{chromatic}^2 \tag{4.9}$$

From Section 4.3, the rise time for the transmitter is 1 ns. The receiver rise time results from its photodetector response and the 3-dB electric bandwidth of its front end (Keiser 1983). The equation for the receiver rise time is given by a standard empirical formula in nanoseconds (Keiser 1983).

$$t_{rx} = \frac{350}{B_{rx}} = 1.25 \text{ ns} \tag{4.10}$$

where $B_{rx}$ = 280 MHz, the 3 dB bandwidth of the receiver.

Because the fiber used in this design is single-mode, the effects of modal dispersion can be neglected.

As discussed in Chapter 2, chromatic dispersion is the combination of material dispersion and waveguide dispersion. By combining equations (2.7), (2.12), and (2.13), the effects of chromatic dispersion can be calculated as

$$t_{mat} = D_{chromatic} \cdot \Delta\lambda \cdot L = 0.7 \text{ ns} \tag{4.11}$$

where $D_{chromatic}$ = $D_{mat} + D_{wg} = +15 + -8 = 7$ ps/nm-km

$\Delta\lambda$ = spectral width of the optical source = 5 nm

L = fiber length = 20 km

After substituting the calculated rise time values into equation (4.11), the calculated system rise time is

$$t_{sys} = 2.95\text{ns} \tag{4.12}$$

As a rule, the total transition time degradation of a link should not exceed 70 percent of the bit period, which is 16 MHz for this design. Therefore, the maximum allowable rise time degradation for the link is 35 ns, much larger than the 2.95 ns calculated in equation (4.12).

The optical components in the system easily handle the 16 MHz Manchester data rate required for the system. The bandwidth of the fiber must be calculated to determine whether the fiber bandwidth limits the system. Equation (2.20) is used for fiber bandwidth calculation, resulting in a maximum attainable bandwidth (Hewlett Packard Co. 1989).

$$BW_{fib} \leq \frac{0.44}{\sqrt{(LD_{modal})^2 + (\Delta\lambda LD_{chromatic})^2}} \tag{4.13}$$

where 0.44 = a constant, assuming the fiber has a Gaussian behavior

L = fiber length = 20 km

$\Delta\lambda$ = bandwidth of source spectrum expressed in nm = 1.2 nm (FWHM)

$D_{modal}$ = the intermodal dispersion of a fiber expressed in ps/km. This only contributes in multi-mode fiber (negligible for single-mode fiber).

$D_{chromatic}$ = the chromatic dispersion of a fiber expressed in ps/nm-km (assume a worst case of 20 ps/nm-km).

Inserting these parameters into equation (4.13) yields

$$B_{fib} \leq 4.4 \text{ GHz} \qquad (4.14)$$

which is easily satisfied for even a worst-case value of $D_{chromatic}$ since the bandwidth of the system is 16 MHz Manchester.

To this point, the optical design of the link is complete, and proper link operation is evidenced.

## 4.10 Link Interface to the Vehicle Electronics

In order to add the design of the fiber optic link into the underwater vehicle, an electronic interface had to be designed on either end of the link to interface the link with the vehicle and launch craft electronics. Figure 4.9 shows the break in the data path between the acoustical A/D converters and the data processors and the recorder.

To verify proper operation of the link design, a recorder is included on both the underwater vehicle and the launch craft. The same data will be recorded on both recorders. At the end of an unsuccessful test, the data from both recorders can be

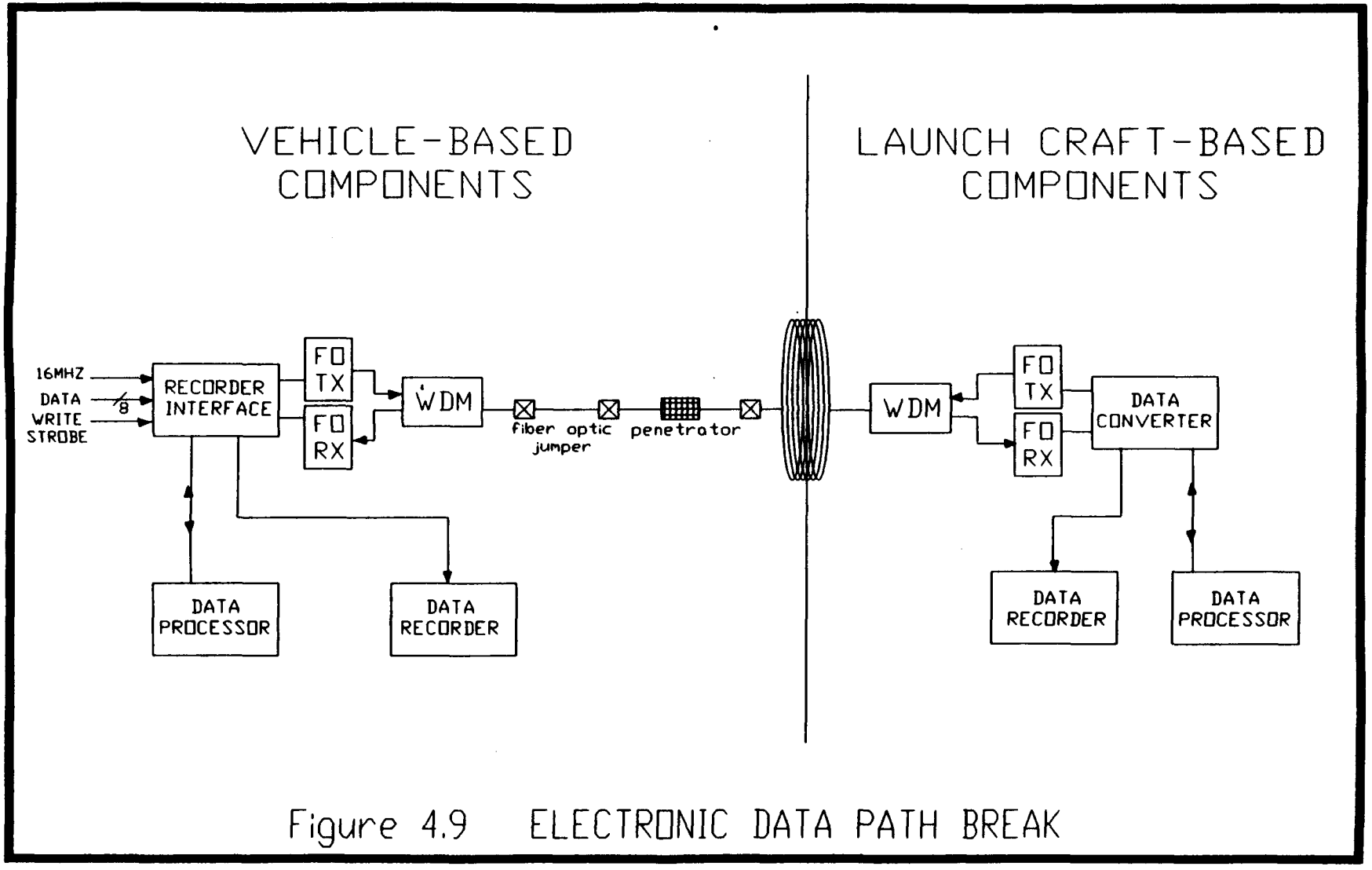


Figure 4.9 ELECTRONIC DATA PATH BREAK

compared to check the communications integrity and to help determine where the failure occurred.

The data processor is also included in both places as a safeguard in case the link does not function properly or the fiber breaks. Safety electronics in the vehicle require continual location and directional commands or it will shut down. The safety electronics keep the vehicle safely within the bounds of the test site and cause the vehicle to shut down if the vehicle approaches a structure or shoreline. If the link malfunctions, the on-board safety electronics will not get vehicle updates from the launch-craft-based data processor, which causes a shutdown. The vehicle-based data processor also processes the data and can provide the necessary updates to keep the vehicle operational.

The design of the vehicle-based card that provides the required interface is called the Recorder Interface Addition. This card has three basic functions: 1) receive data from the vehicle electronics and input the data to the fiber optic link for transfer up the link, 2) receive data from the vehicle electronics and input the data to the recorder, and 3) receive the optical data from the launch craft and provide the data to the vehicle data processor and recorder.

### 4.10.1 Data Flow from the Vehicle to the Launch Craft

The interface between the vehicle electronics and the Recorder Interface Addition consists of eight bits of parallel data at 2 Mbytes per second, a 2 MHz write strobe in sync with the data, and a 16 MHz clock signal in sync with the data.

Since the original data path was broken between the vehicle electronics and the recorder, the interface for the Recorder Interface Addition is the same as that for the recorder, 8-bit parallel data at 2 Mbytes/second. As such, the data and write strobe are sent through buffers and signal conditioners right to the recorder.

The data to the optical transmitter must be converted to the serial, ECL-level bitstream data format required by the transmitter. The parallel data is first converted into a 16 Mbps bitstream using a parallel-to-serial converter and the 16 MHz clock.

The serial bitstream is then converted to a Manchester code. The Manchester code is an RZ format that is obtained from a direct modulo-2 addition of the serial data and the 16 MHz clock. This Manchester format requires only one line to carry both the data and a synchronized clock signal. The Manchester code also helps eliminate DC and low frequency noise and prevents possible receiver saturation during the transfer of all logical 1's in the case of NRZ data.

The Manchester-encoded serial bitstream is then passed through a TTL-to-ECL converter. The optical transmitter requires an ECL-level bitstream to maintain a high data rate. The ECL-level bitstream is then input to the transmitter for transfer up the fiber optic link.

### 4.10.2 Data Flow from the Launch Craft to the Vehicle

The format for the data from the Recorder Interface Addition to the on-board data processor is a serial RS-232 bitstream. The optical receiver receives optical signals from the launch craft. The receiver outputs an ECL-level, Manchester-encoded bitstream to the Recorder Interface Addition.

This bitstream is first passed through an ECL-to-TTL converter. The new TTL-level bitstream is the input to a Manchester decoder. The decoder separates the data from the 16 MHz clock and outputs the 16 Mbps bitstream in sync with the clock. This bitstream is then clocked into a TTL-to-RS-232 translator. The bitstream is converted to an RS-232 signal and output to the data processor.

## 4.11 Link Interface to the Launch Craft Electronics

### 4.11.1 Data Flow from the Vehicle to the Launch Craft

The Data Converter is the card designed to provide the interface between the fiber optic link and the launch-craft-based recorder and data processor. This card receives a Manchester-encoded, ECL-level bitstream, representing the fiber optic vehicle data, from the fiber optic receiver.

The ECL-level bitstream is passed through an ECL-to-TTL converter for conversion to TTL levels. The new TTL-level bitstream is input to a Manchester decoder. The decoder separates the data from the 16 MHz clock and outputs the

16 Mbps bitstream in sync with the clock. This bitstream is split and sent in two directions, to the data processor and to the recorder.

The bitstream to the data processor is input to a TTL-to-RS-232 translator and is converted to an RS-232 signal and output to the data processor.

The bitstream to the recorder is first sent to a serial-to-parallel converter and converted to an 8-bit parallel data byte. The 16 MHz clock is divided down to a 2 MHz write strobe and sent with the data to the data recorder. The parallel data and the write strobe is also sent to a test fixture called the Quicklook Box.

The Quicklook Box provides the capability of seeing the acoustic data in real time. The data in the vehicle is formatted into 32-Kbyte data blocks for recording purposes. Each block of data is headed by an 8-byte frame alignment word. This frame alignment word is used by the Quicklook Box and data analysis equipment to detect the beginning of each new data block. Once the frame alignment word is detected, the selected channels of acoustical data are stripped out and input to an oscilloscope or a personal computer (PC). This enables the operator to determine if the test is valid while it is ongoing. If the data from the vehicle is not valid, the operator can shut down the test and evaluate any problems. Figure 4.10 shows the 32-Kbyte data block.

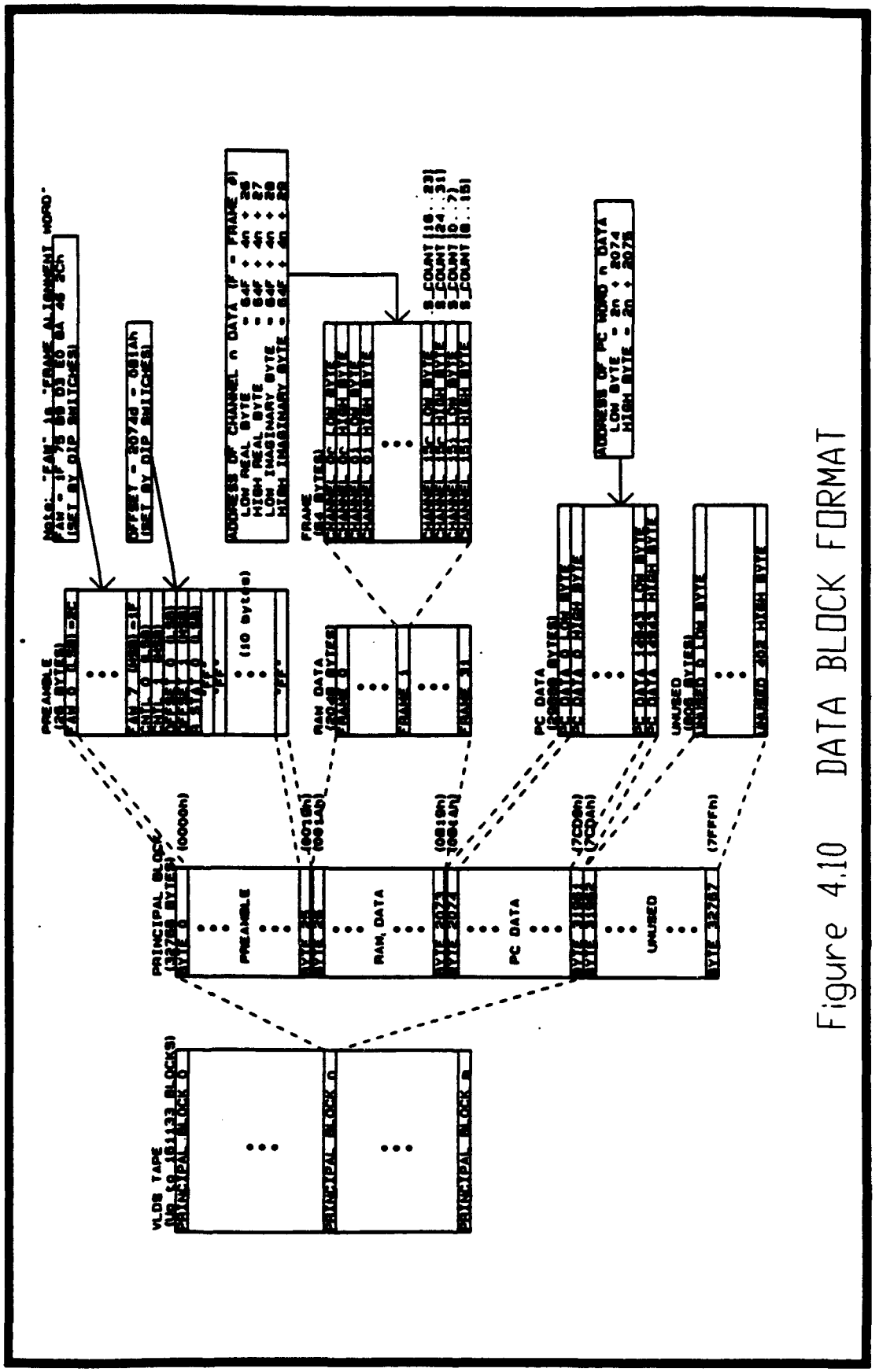


Figure 4.10 DATA BLOCK FORMAT

### 4.11.2 Data Flow from the Launch Craft to the Vehicle

The Data Converter card also handles the data flow from the launch-craft-based data processor to the underwater vehicle. The data from the data processor is sent down the link to the safety and guidance circuitry located in the vehicle. This data provides direction and location data to the safety electronics and issues steering commands to the guidance electronics. The data is also included in the data format recorded by the recorders on both the vehicle and the launch craft.

The data from the data processor is a serial, RS-232 bitstream. The data is passed through an RS-232-to-TTL translator and then input to a Manchester encoder. Here, the data is combined with a 16 MHz clock into a Manchester-encoded bitstream. This bitstream is input to a TTL-to-ECL converter and converted to ECL levels. This ECL data is input to the 1300 nm optical transmitter and transferred down the link to the underwater vehicle.

# Chapter 5

# TESTING

This chapter describes the tests performed to verify operation of the link. Section 5.1 describes the laboratory tests performed at ARL Penn State, and Section 5.2 describes the in-water field tests performed at a remote test site. For all tests, a 20 km spool of fiber was used. Chapter 6 provides a discussion of the test results.

## 5.1 Laboratory Testing

### 5.1.1 Serial Character Transmission Test

The system configuration for the serial character transmission test is shown in Figure 5.1. The configuration consists of opposite ends of the fiber optic link connected to the serial ports of two PCs. Both PCs run a data transfer utility software package called Fastlynx, Version 1.02, from Rupp Corporation. Fastlynx provides the capability of transferring small or large quantities of data between PCs using either the serial or parallel port. This package also offers both serial and parallel port tests, where serial streams or large blocks of parallel data are sent from one PC to the other and verified for correctness.

The serial character transmission test is a serial port test in which one PC sends the sentence "The quick red fox jumped over the lazy brown dogs back!" to the other PC in a serial RS-232 format stream. The data transfer is simultaneous and bidirectional, such that while one PC is transferring data, it is also receiving data from the other PC.

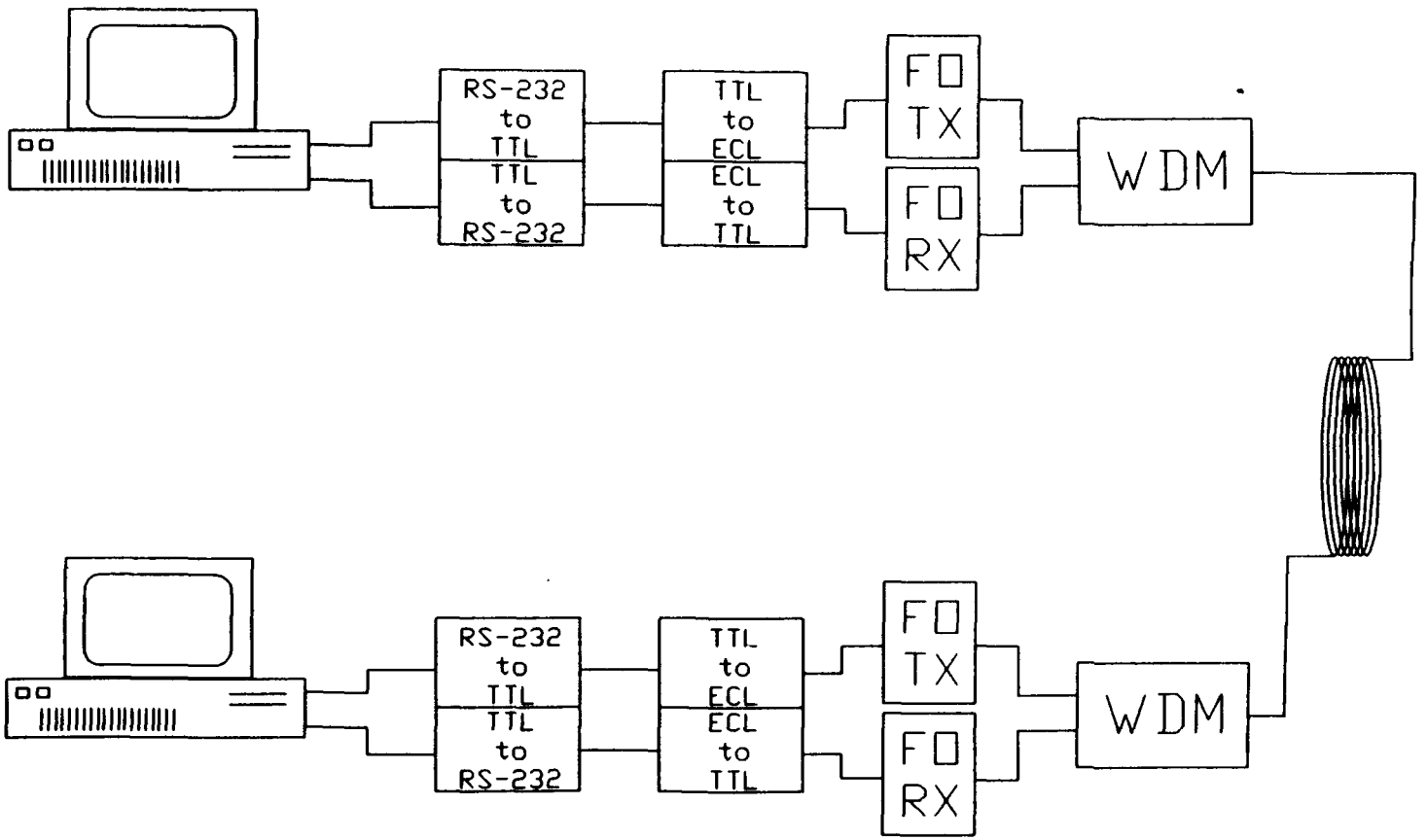


Figure 5.1 SERIAL CHARACTER TRANSMISSION TEST CONFIGURATION

The test is initiated by running the Fastlynx software on both PCs and selecting the "Serial Character Transmission Test" option from the Diagnostics menu. At this point, the screens of both PCs should resemble the screen in Figure 5.2. The top box in this screen indicates the characters being sent and the lower box represents the characters received. If the link and PCs are functioning properly, each PC will continue to send and receive the characters shown in Figure 5.2 until the test is terminated by the user. If an incorrect character is received, it is omitted from the display. The screen on the receiving PC displays only the received characters that were correct, as shown in Figure 5.3.

The screens shown in Figures 5.2 and 5.3 are from actual tests. The errors shown in Figure 5.3 were induced by disconnecting the link. The results of this test verify the link's simultaneous, bidirectional data transmission capabilities.

### 5.1.2 Byte Block Transmission Test Configuration

The link configuration for the Byte Block Transmission Test is the same as shown in Figure 5.1. Like the Serial Character Test, this test also uses Fastlynx software, but the "Block Transmission Test" option is selected. For this test, a "master" PC sends serial blocks consisting of 8192 (8K) bytes of data in RS-232 format to a "slave" PC. The slave PC performs error checking on the blocks to verify accurate transmission of data and sends the results back to the master PC. The master PC logs the errors (if any) and a parameter called Timeout. This parameter indicates that the master PC did not receive the results of the previous data block from the slave PC in the allotted time.

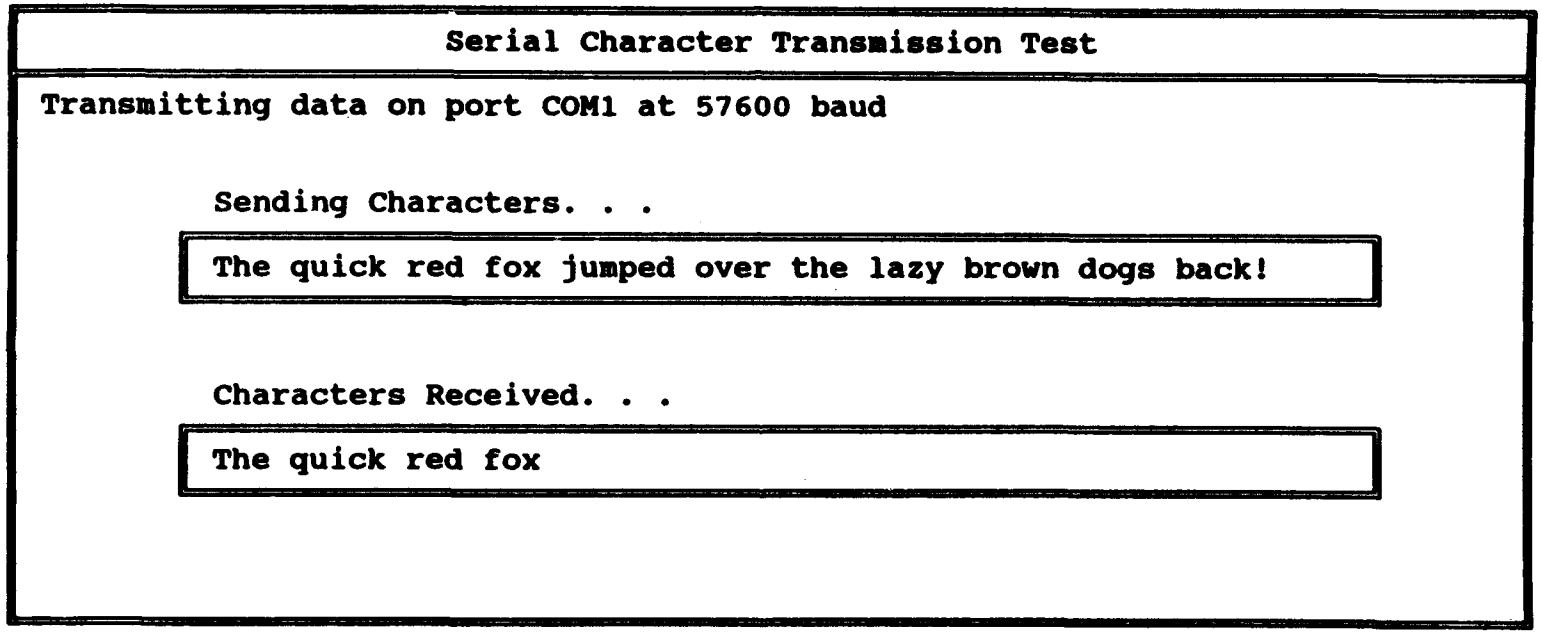


Figure 5.2 SERIAL CHARACTER TRANSMISSION TEST SCREEN

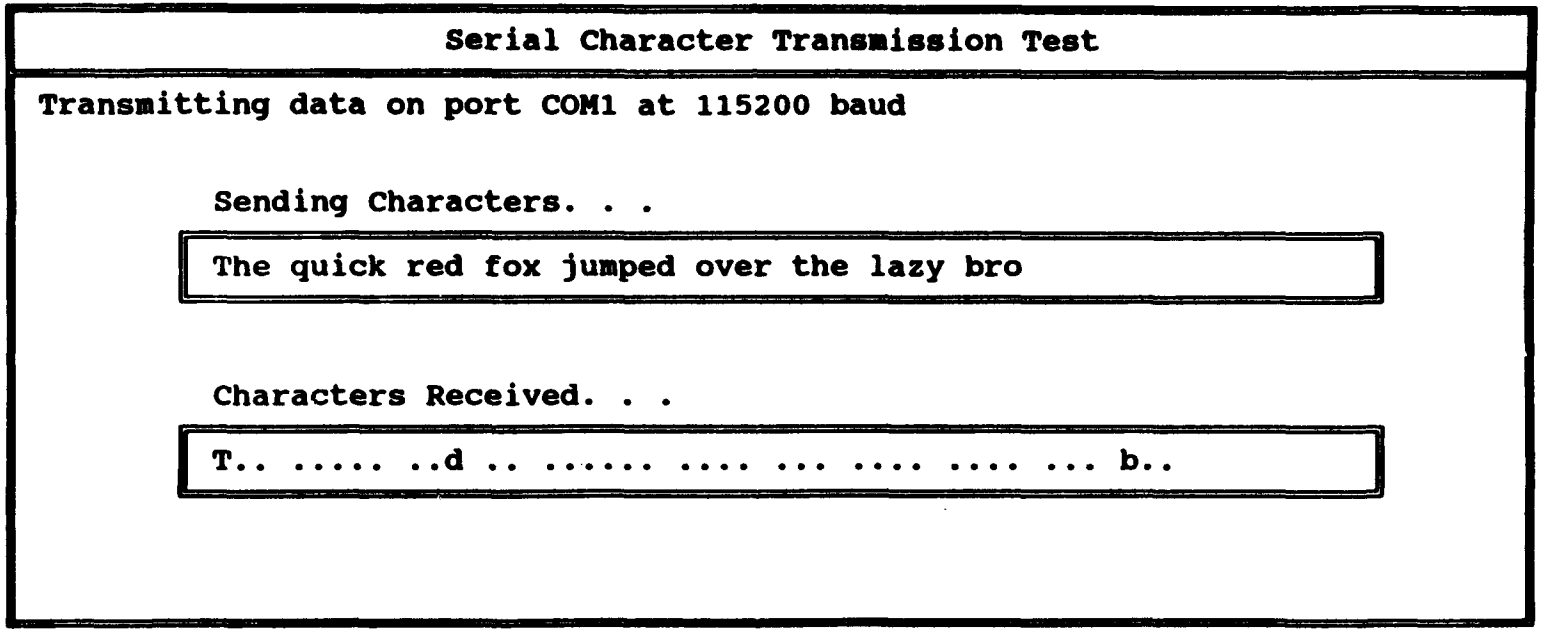


Figure 5.3 SERIAL CHARACTER TRANSMISSION TEST ERRORS

To initiate the test, a master PC and a slave PC are selected. Both PCs run the Fastlynx software. However, the master PC selects the "Block Transmission Test" option; the other PC automatically switches to slave mode. The master PC begins sending 8-Kbyte blocks of data to the slave computer. Figure 5.4 shows the master PC screen, indicating the number of bytes transferred and any errors. The master PC continues to transfer blocks of data to the slave PC until the system is halted by the user.

The "Block Transmission Test" verifies transmitted data integrity and provides insight into the designed $10^{-9}$ BER of the system. To achieve this BER, $1x10^9$ bits must be transmitted with only one error. The master PC logs an error if a byte of data was not received correctly. It does not log how many bits in the byte were bad. Because errors are not logged to the individual bits, an exact BER cannot be determined from this test.

Figure 5.5 shows that 82,575,360 bits of data transferred without an error. To determine a BER, this test was repeated until over $1x10^9$ bits were transferred. During the BER test, one error occurred, and that screen is shown in Figure 5.6. The numbers on the screen in the "Elapsed seconds" and "Speed" columns are not correct because the maximum time resolution of the program was exceeded for the test. The error logged was not necessarily a link error. The transmitting or receiving PC might have caused the error. Also, it is not known whether the error was more than one bit. Assuming the error to be a single-bit link error, the BER of the link was verified since only one error occurred in more than $1x10^9$ bits.

**Block Transmission and Auto Port Select Test**

Port : COM1(57600+)
Cable Type: Serial, 7-wire

Auto Port Select - Pass: 126 Fail: 0

| Operating Speed | Error Checking | Bytes Transferred | Elapsed Seconds | Speed bytes/sec | Error Count | Timeout Count |
|---|---|---|---|---|---|---|
| Slow | CRC | 57344 | 6.113 | 9380 | | |
| Slow | Checksum | 57344 | 6.066 | 9453 | | |
| Normal | CRC | 57344 | 6.118 | 9372 | | |
| Normal | Checksum | 57344 | 6.068 | 9450 | | |
| Turbo | CRC | 57344 | 6.126 | 9360 | | |
| Turbo | Checksum | 57344 | 6.073 | 9442 | | |

Figure 5.4 BYTE BLOCK TRANSMISSION TEST SCREEN

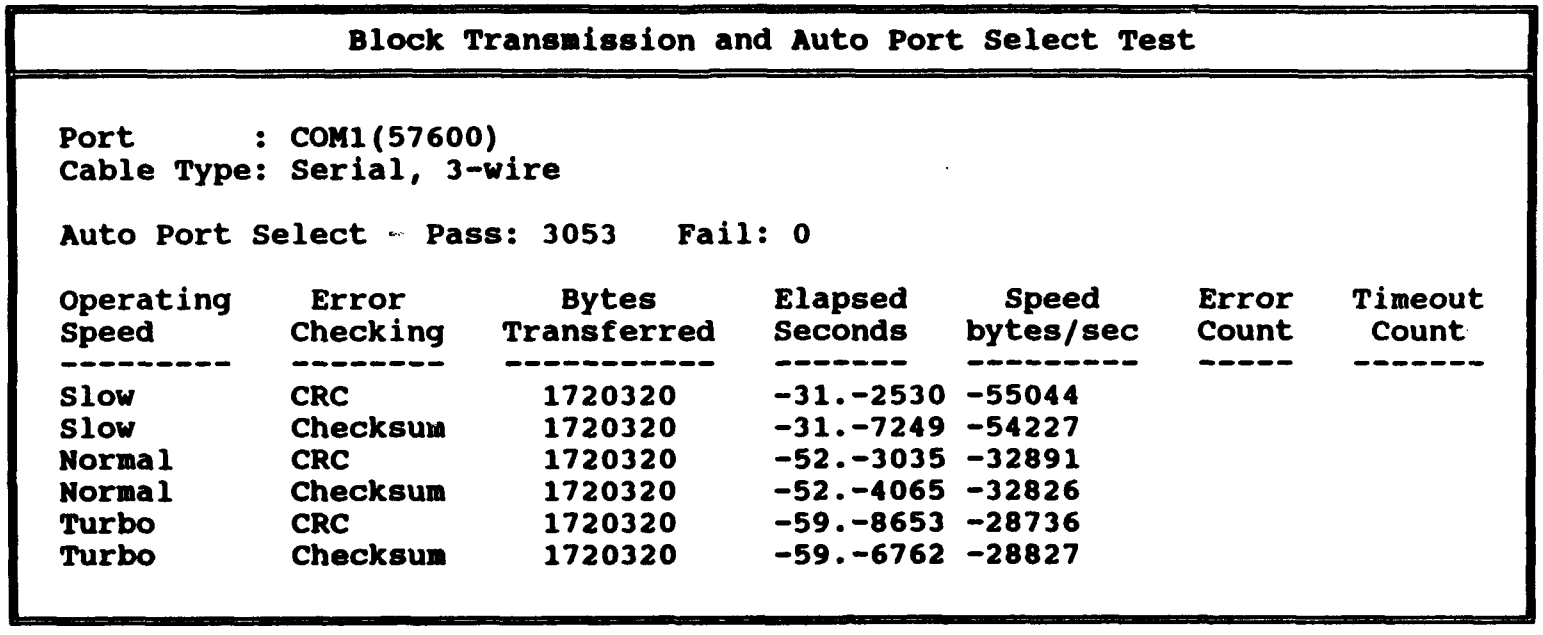


Figure 5.5 DATA SCREEN FOR TRANSMISSION OF 8Mbits OF DATA

**Block Transmission and Auto Port Select Test**

Port : COM1(57600+)
Cable Type: Serial, 7-wire

Auto Port Select - Pass: 988 Fail: 12

| Operating Speed | Error Checking | Bytes Transferred | Elapsed Seconds | Speed bytes/sec | Error Count | Timeout Count |
|---|---|---|---|---|---|---|
| Slow | CRC | 573440 | 90.231 | 6355 | | |
| Slow | Checksum | 524288 | 80.550 | 6508 | | |
| Normal | CRC | 516096 | 73.681 | 7004 | | |
| Normal | Checksum | 516096 | 73.415 | 7029 | | |
| Turbo | CRC | 516096 | 71.682 | 7199 | | |
| Turbo | Checksum | 516096 | 74.447 | 6932 | 1 | |

Figure 5.6 BER TEST ERROR SCREEN

Results of this test indicate that large quantities of data can be sent across the link with minimal error. Also, the system BER approaches or even exceeds the $10^{-9}$ BER design goal. This test also verifies data flow from the data processor (in this case a PC), through the Recorder Interface, up the fiber optic link, through the Data Converter, and to the other data processor (another PC).

### 5.1.3 Anechoic Tank Test

To facilitate the testing, measuring, and calibrating of transducers and transducer arrays, ARL Penn State maintains an anechoic acoustic test tank. Data measured in the tank includes frequency response characteristics, directivity patterns, and impedance and admittance properties over a frequency range of 1 kHz to 500 kHz. Pulse gating of signals to sound projectors and from receiving hydrophones permits measurement of transmitted sound levels before arrival of the first ambient reflection. The tank is 26' x 17.5' x 18' and has acoustic-absorbing materials on the tank walls to reduce reverberation.

For this test, the front-end electronics section of the vehicle, including the link and payout fiber, was mounted on a bracket and lowered into the anechoic tank, as shown in Figure 5.7. The vehicle was powered as if under normal operation, and a sinusoidal waveform was transmitted into the water by an underwater sound projector. This waveform was received by the vehicle sonar, conditioned, digitized, and assembled into a 32-Kbyte data block for transmission up the link. At the other end of the link, the 32-Kbyte data block was sent to the Quicklook Box, where the acoustic data was stripped out and stored in a PC. A PC-based Matlab plotting routine was used to plot

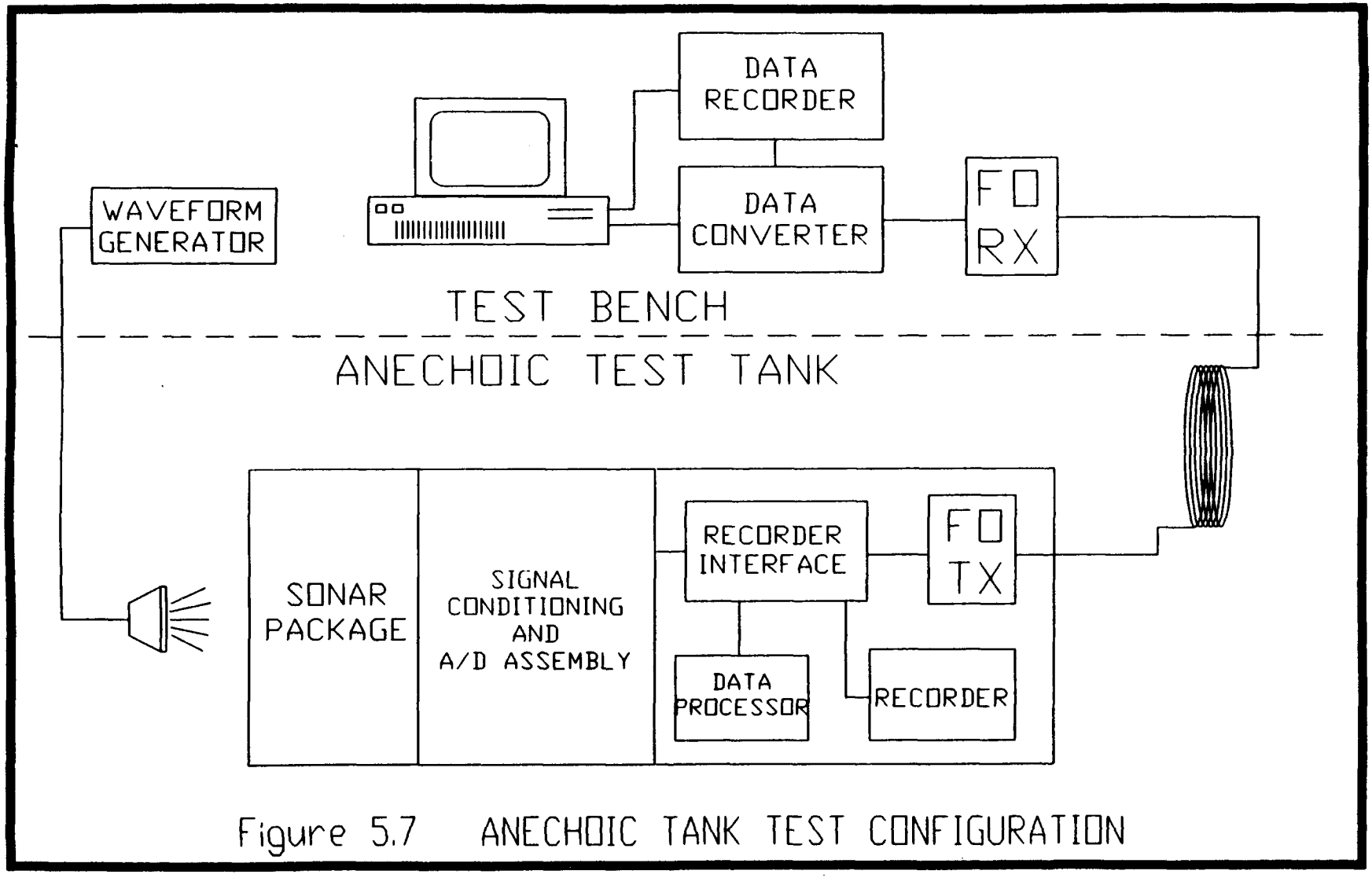


Figure 5.7 ANECHOIC TANK TEST CONFIGURATION

the data. Figures 5.8 and 5.9 show the real and imaginary components of the sinusoidal data. The "Samples" label on the horizontal axis indicates the number of data blocks sampled for the plot. Figures 5.8 and 5.9 very accurately model the waveform input into the tank.

Results from this test verify the design of the fiber optic link into the underwater vehicle. These results also indicate that recording can be accomplished on the launch craft, allowing the recorder to be removed from the vehicle.

### 5.1.4 Ramp Data Test

The configuration for this test is shown in Figure 5.10. The "underwater" portion of the vehicle is set up to receive data from the "launch craft" equipment. As mentioned in Section 4.10, data from the launch-craft-based data processor is sent down the link and included in the 32-Kbyte data block as PC data (see Figure 4.10). This block is recorded in the vehicle and also transmitted up the link for recording on the launch craft.

For this test, the launch-craft-based PC runs a software program to generate ramp data. The ramp data is sent down the link to the vehicle, where it is packaged into the recorded 32-Kbyte data block. The vehicle recorder is connected to the Quicklook Box, where the ramp data is extracted and stored in the PC. A Matlab plotting routine is used to plot the stored data. Figure 5.11 shows the plot of the ramp data.

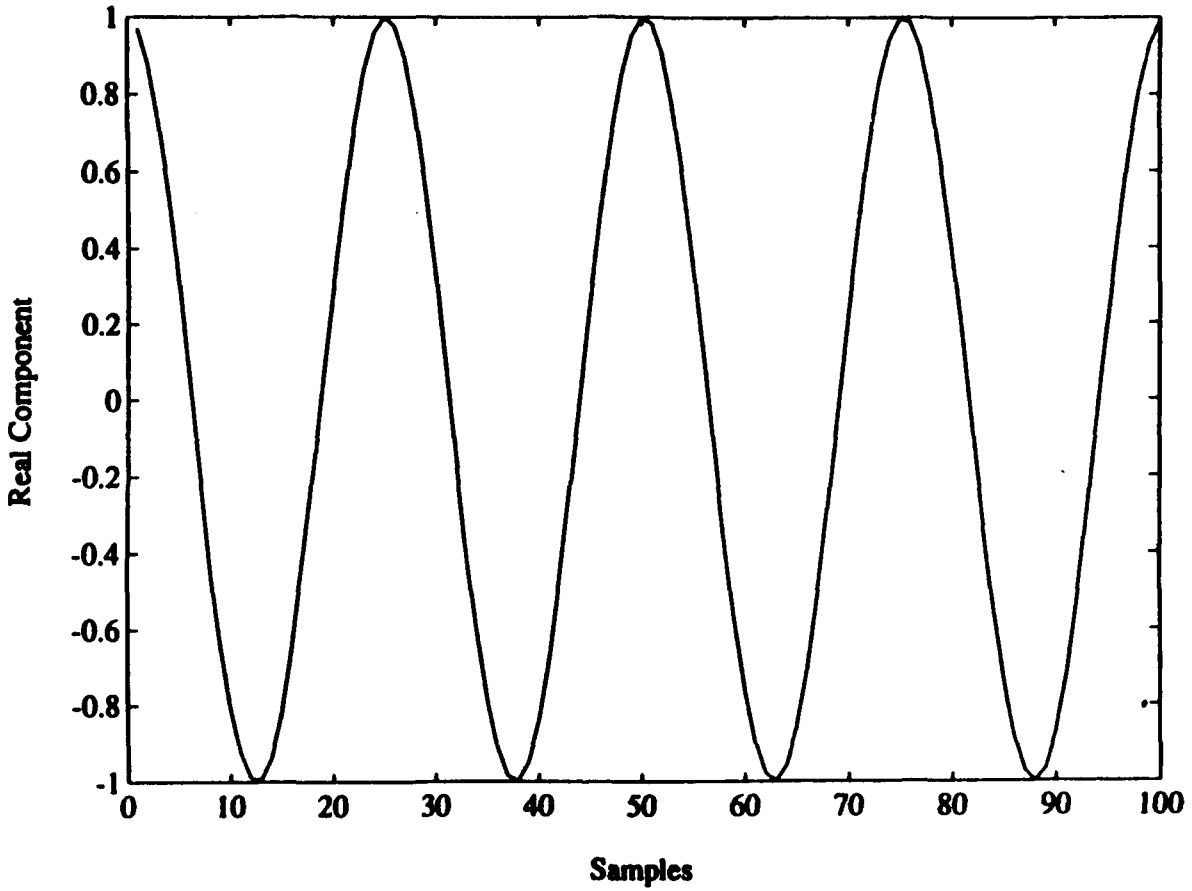


Figure 5.8 REAL COMPONENT OF SINUSOIDAL TANK TEST DATA

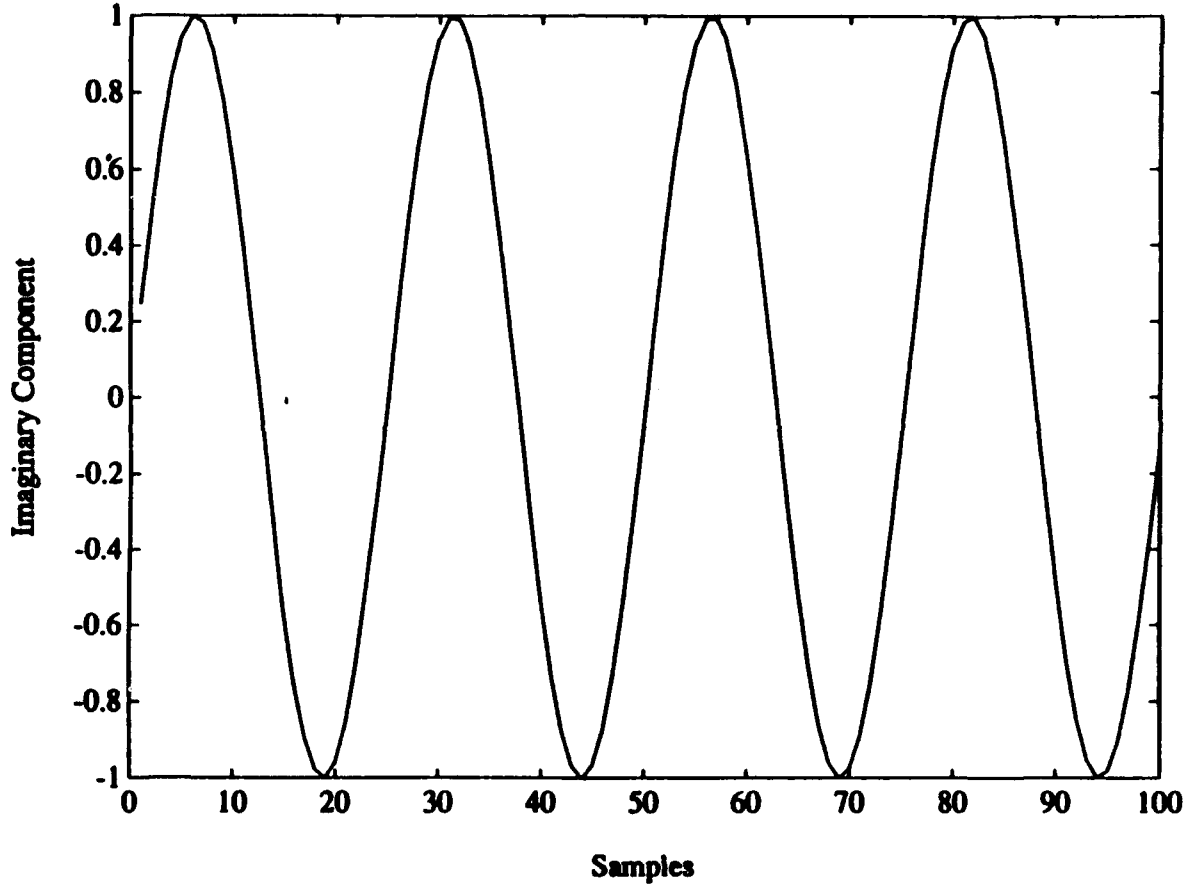


Figure 5.9 IMAGINARY COMPONENT OF SINUSOIDAL TANK TEST DATA

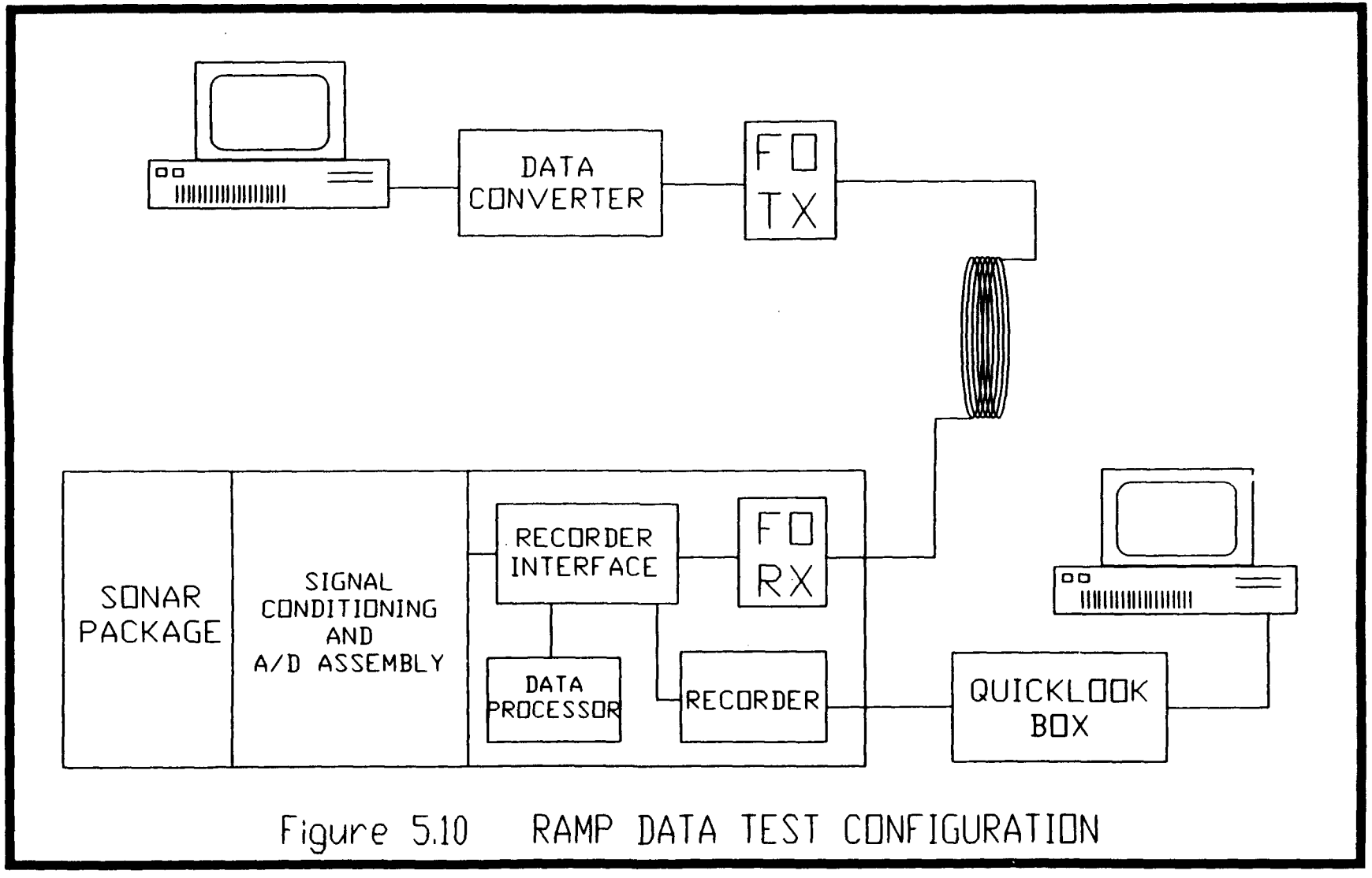


Figure 5.10 RAMP DATA TEST CONFIGURATION

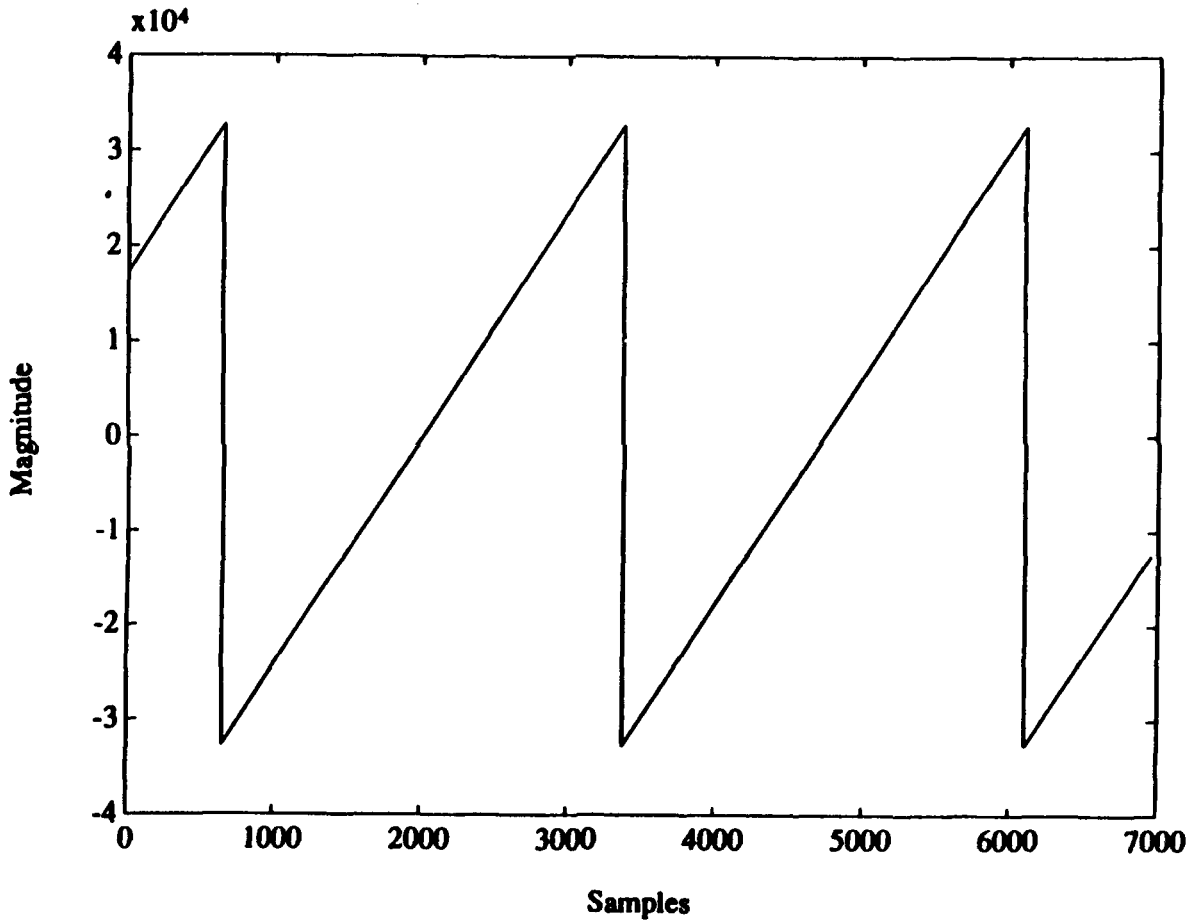


Figure 5.11 PLOT OF DATA FOR RAMP DATA TEST

Results from this test verify the link operation with vehicle components and also verify the data flow from the launch craft to the vehicle. This test also indicates data processing capabilities in the launch craft since data from the launch craft data processor was accurately sent down the link and recorded.

The Ramp Data Test concludes all laboratory tests for the link. Results of these tests indicate proper operation of the link and the functioning of the vehicle/launch craft components together as a system. Design objectives met as a result of the laboratory tests include:

- simultaneous, bidirectional communication
- BER of $10^{-9}$
- link operation with vehicle electronics
- data processing and recording capabilities on the launch craft

The remainder of the tests for the link and associated components are actual underwater field tests.

## 5.2 Field Tests

For field tests, the underwater vehicle is shipped to an outdoor test range. The range is specifically designed to accommodate testing of a variety of underwater vehicles, from large manned underwater vehicles to the smaller AUVs. Like the anechoic tank, this test range is equipped with sound projectors and hydrophones. Underwater electronics track the vehicle under test during an experiment. The range is also equipped with surface ships to launch and retrieve the vehicles under test.

The vehicle/link configuration for the field tests is shown in Figure 5.12. The vehicle is mounted in a launch cage and lowered over the side of the launch craft into the water. After completion of self-tests, the vehicle is launched from the cage. The vehicle maneuvers down range, and the sonar listens to select volumes of the water. The sonar data is conditioned, digitized, and packaged into data blocks as shown in Figure 4.10. These data blocks are recorded on the vehicle and on the launch craft. The sonar data in the data blocks is processed by the launch-craft-based data processor. Based on the sonar data, steering commands are sent to the vehicle to direct it toward the acoustic source.

Successful tests are complete when the vehicle operates for the duration of the experiment and surfaces, or when all fiber has been payed out and the vehicle surfaces. Unsuccessful tests occur when the vehicle surfaces before the experiment run time has elapsed and it does not locate or track the acoustic source. Examples of system problems resulting in unsuccessful runs are broken fiber, loss of system power, and lack of correct direction or steering information. Eight tests were performed on the vehicle and link. Five tests were considered successful, as the vehicle located the acoustic source, and three tests were unsuccessful. In two of the three unsuccessful tests, the fiber broke, and the third failure was caused by internal vehicle problems not related to the link.

Figure 5.13 is a range plot of a successful field test. The launch-craft data processor generated the steering commands to direct the vehicle toward an acoustic

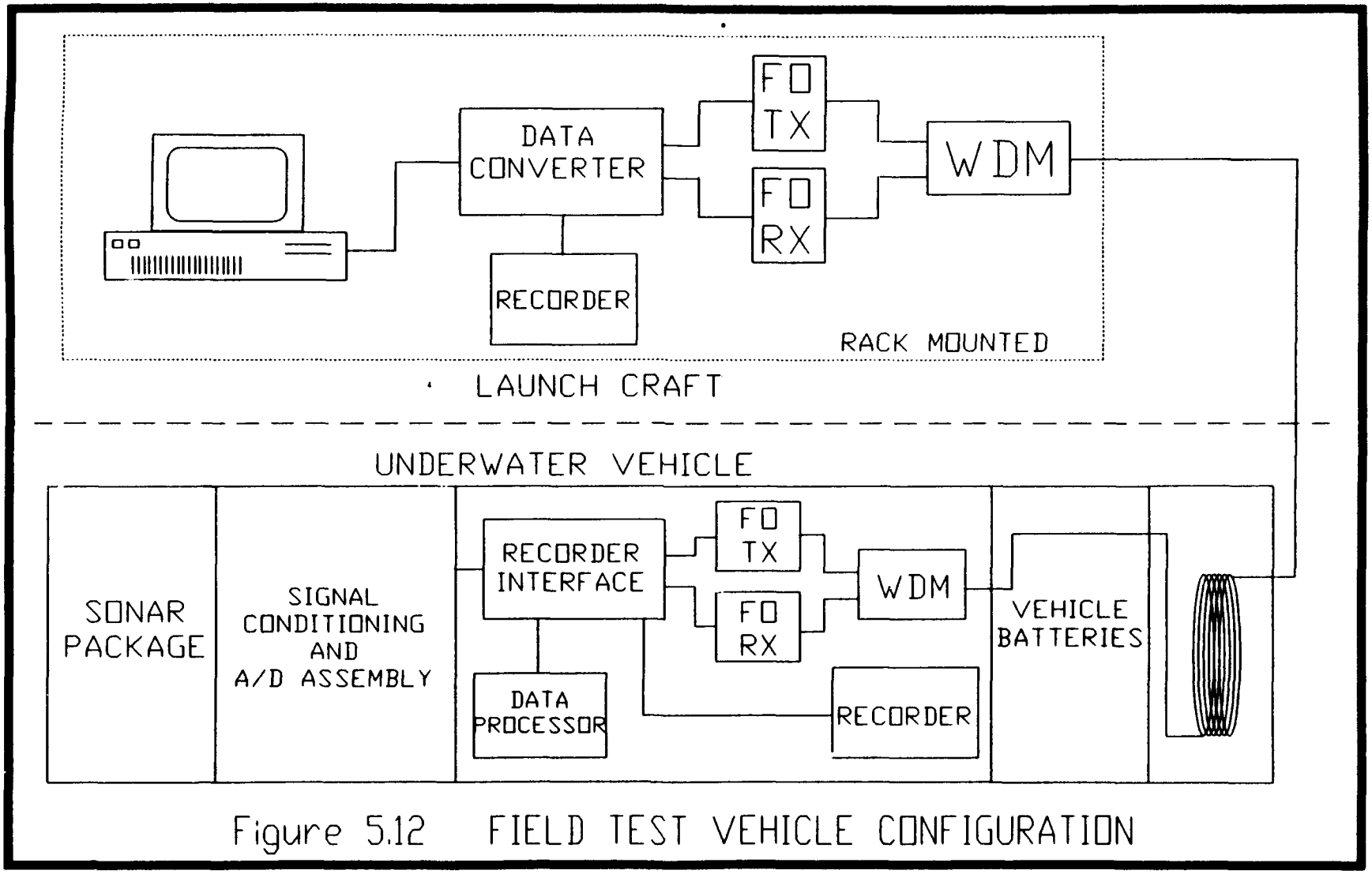


Figure 5.12 FIELD TEST VEHICLE CONFIGURATION

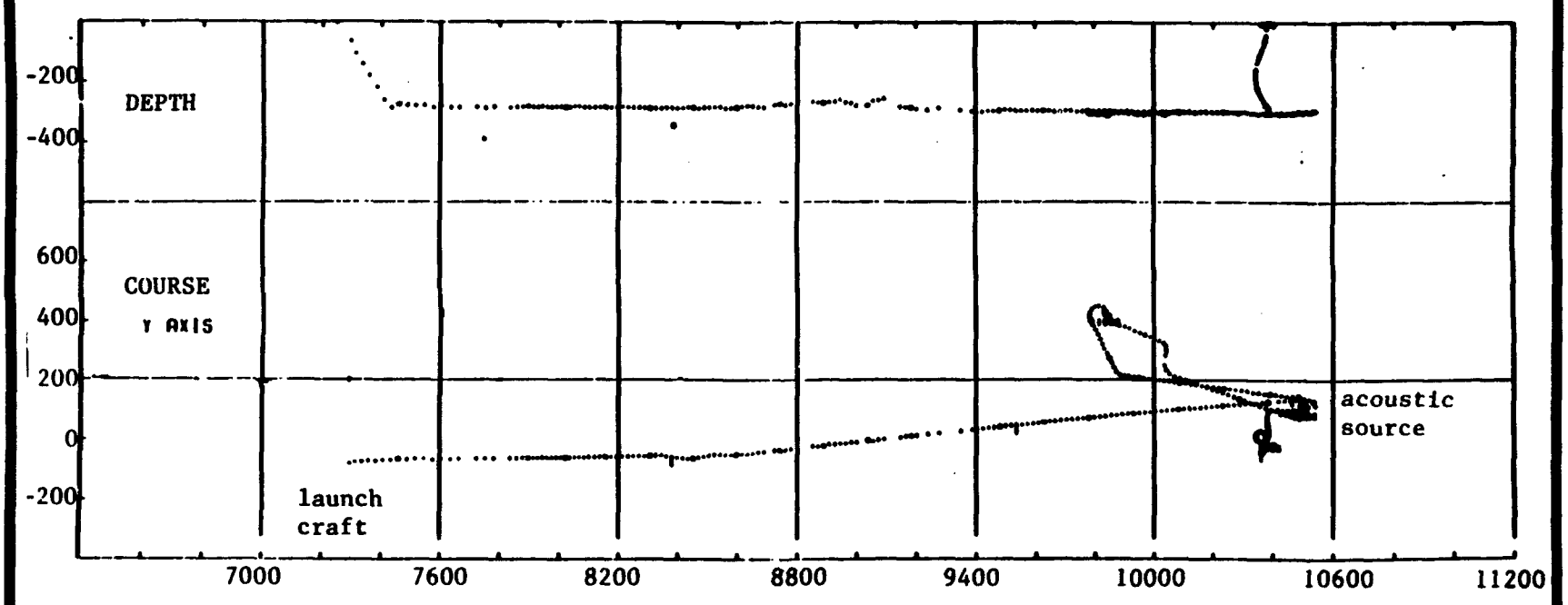


Figure 5.13 RANGE PLOT OF FIELD TEST

source located down range based on the received sonar data. Figure 5.13 consists of two plots: 1) the course, and 2) the depth of the vehicle as it traveled down range.

Referring to Figure 5.13, the vehicle traveled down range approximately 1500 yards, detected the acoustic source, and turned left toward the source. The vehicle stayed on this course for another 2000 yards, where it encountered the acoustic source, maneuvered around the source, turned, and proceeded to travel down range. The vehicle continued traveling down range for about 1000 yards and turned to reacquire the acoustic source. Once the acoustic source was detected, the vehicle headed down range and converged on the source. Experiment time expired after the vehicle passed the source a second time, and the test ended with the vehicle going to the surface.

To verify launch-craft-based recording capabilities, the PC data in the 32-Kbyte data blocks recorded on the launch craft data recorder was stripped out and stored in a PC. This data represents the steering and directional commands transmitted from the launch-craft-based data processor to the vehicle. This data indicates the vehicle's version of its path as it travelled down the test range. Figure 5.14 is a plot of the PC data. A comparison of Figures 5.13 and 5.14 demonstrates on-board recording capabilities because the data recorded on the launch craft very accurately models the plot from the test site facility.

Results of this test verify operation of the fiber optic link as designed into the underwater vehicle. This test also demonstrates on-board data processing and recording capabilities. The launch-craft-based data processor generated steering commands, based

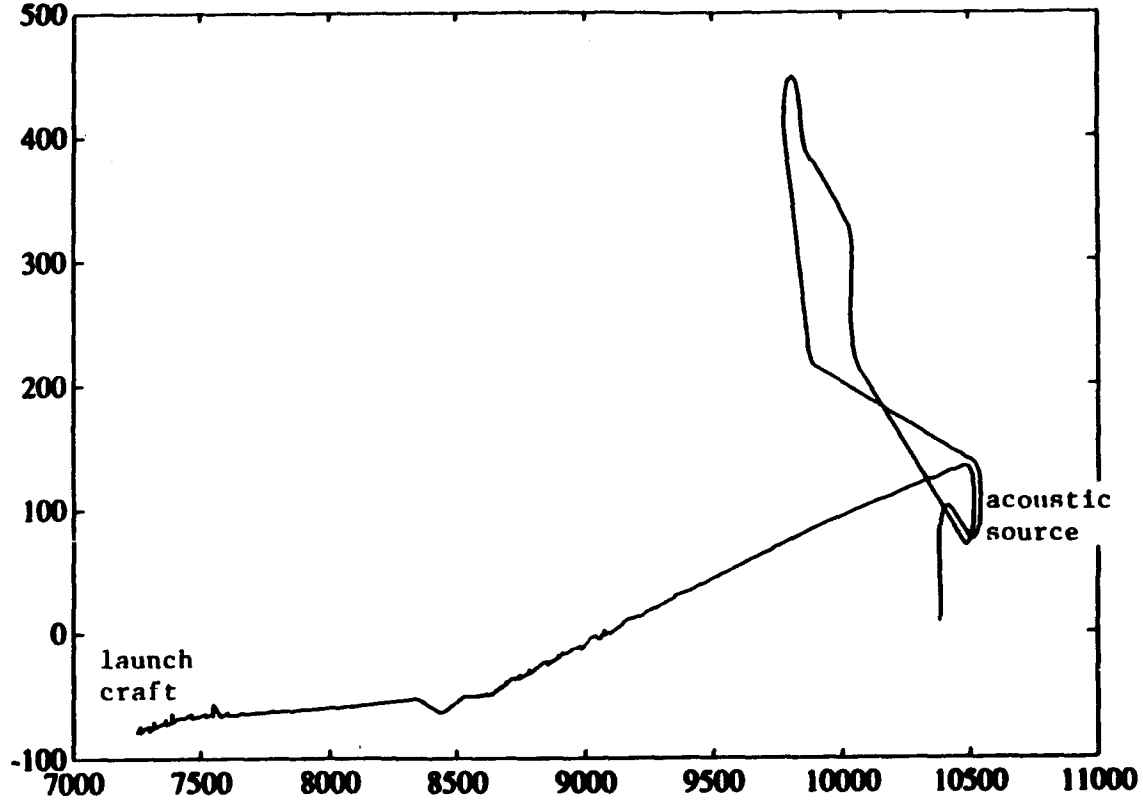


Figure 5.14 PLOT OF VEHICLE FIELD TEST DATA

steering commands for future data analysis and for verification of correct decision making by the data processor.

After successful completion of both laboratory and field tests, no further tests were performed on the vehicle. Results of the tests satisfied all original design objectives. The link and associated vehicle were considered fully operational and ready for future use.

# Chapter 6

# DISCUSSION OF TEST RESULTS

The following discussion summarizes the tests performed on the fiber optic link and lists the design objectives that were verified by these tests.

## 6.1 Serial Character Transmission Test Results

The test configuration consisted of connecting the serial ports of two PCs together using the fiber optic link. The link replaced a seven-conductor wire cable. Fastlynx software prompted each PC to simultaneously transmit serial RS-232 data across the link to the other PC.

Results of this test verified the simultaneous, bidirectional data transfer capabilities of the link. This test also confirmed the ability of the Recorder Interface Addition and the Data Converter to interface to a computer using a serial, RS-232 data format.

## 6.2 Byte Block Transmission Test Results

This test used the same configuration as the serial character transmission test; however, the Fastlynx software caused a master PC to generate and transmit data blocks consisting of 8192 bytes to a slave PC. The slave PC checked the data blocks for errors and returned the results to the master PC.

Results of this test demonstrated that large amounts of data can be transmitted across the link with minimal errors, and they indicate that the BER of the system meets or even exceeds the $10^{-9}$ goal. Because this test required the transfer of large quantities of data, it also verified the ability of the link to be operational for long periods of time.

## 6.3 Anechoic Tank Test Results

The configuration for this test required the vehicle electronics, including the vehicle-based fiber optic link components, to be lowered into an anechoic test tank. The launch craft electronics and link components were located on a test bench above the tank. A sinusoidal tone was injected into the water, received by the sonar, conditioned, digitized, and sent up the link to the Quicklook Box, where it was stripped out and stored in a PC. This sonar data was plotted using a PC-based Matlab plotting routine.

Results of this test verified the ability of the Recorder Interface Addition and the Data Converter to interface to the vehicle's A/D Assembly and the recorder's parallel data bus. The Quicklook Box requires the same parallel interface as the recorder. Sending parallel data to this test box is the same as sending data to the recorder. As such, this test also verified the capability to record data at the launch craft.

## 6.4 Ramp Data Test Results

The configuration for this test consisted of the launch craft data processor (PC) connected through the link to the underwater portion of the vehicle. A program in the PC generated ramp data that was sent down the link and included in the 32-Kbyte data

block recorded in the vehicle. The data block was sent from the recorder to the Quicklook Box, where the ramp data was stripped out and stored in a PC. A PC-based Matlab plotting routine was used to plot the data.

Results of this test demonstrated the capability for the launch-craft-based data processor to generate and transmit data to the underwater vehicle. This indicates the ability to achieve launch-craft-based data processing for steering the vehicle toward an acoustic source. This test also verified vehicle-based record capabilities through the Recorder Interface Addition.

## 6.5 Field Test Results

The configuration for this test is a launch craft, housing all launch craft electronics and link components to launch the underwater vehicle, incorporating all vehicle electronics and link components. The vehicle traveled down the test range listening (with sonar) for an acoustic source. The sonar data from the vehicle was sent up the link to the launch-craft-based data processor, where steering commands were generated. The commands were sent back to the vehicle, directing it toward the acoustic source. The steering commands were also recorded on the vehicle for future processing and data analysis. There were a total of eight field tests.

Two very important objectives met with these tests that were not fully satisfied with previous tests are: 1) demonstration of full-link operation within the vehicle during an actual experiment, and 2) achievement of launch-craft-based data processing and recording.

# Chapter 7

# CONCLUSION

The goal of this fiber optic project was to design a fiber optic link between an underwater vehicle and its launch craft. A fiber optic link was selected over the traditional copper wire transmission medium because it offers the advantages of a wider bandwidth, lower attenuation losses, less weight, and a smaller diameter than its copper counterpart.

Fiber optic technology has the potential to permit error-free, simultaneous, multi-directional communication at high data rates for long distances without the use of repeaters. This capability provides the option of moving the data processing and recording equipment from the underwater vehicle to its launch craft, allowing for greater data processing capacities, reducing both the size and weight of the vehicle and minimizing power consumption. Through this reduction in power requirements, increased experiment durations can be realized.

The design of the fiber optic link for the underwater vehicle consisted of 1) specifying the following optical components:

- transmitter pair
- WDM
- optical bulkhead penetrator
- fiber optic cable
- fiber optic connectors

and 2) designing the electronics essential for interfacing the optical link components to the existing electronics in the vehicle and the launch craft.

The design of the link into the vehicle was a success because all of the following design objectives for the link were achieved.

- The capability of simultaneous, bidirectional communication across an optical fiber linking an underwater vehicle and its launch craft
- The capability of transmission distances ranging up to 20 km
- The design of the link into a vehicle while minimizing mechanical changes to the vehicle
- The capability of moving the recorder in the vehicle to the launch craft so that vehicle data is recorded on the launch craft
- The capability of moving the data processor in the vehicle to the launch craft so that vehicle data is processed on the launch craft

These objectives were demonstrated in both lab and integrated field tests. The field tests were the most inclusive tests as they involved launching the vehicle, incorporating the fiber optic link, from a surface ship on an outdoor test range designed for underwater vehicle tests. During a successful test, the vehicle acquired an acoustic source using a data processor, located on the launch craft, based on sonar data from the vehicle.

At present, the link design is in use for a number of lab and field test experiments. With the link firmly in place, increased data processing capabilities are

being investigated. Because a large amount of space is available on the launch craft, larger processing systems can be added to replace the single-board processors used in the past. The increased data rates of the larger processing systems are easily handled by the current link design.

Other applications being considered for this link are an increase in the separation capabilities of the vehicle from the launch craft beyond 20 km and adding a human interface on the launch craft to generate the steering commands based on data from the vehicle displayed on a computer terminal.

# REFERENCES


Agrawal, G. P., Fiber Optic Communication Systems, John Wiley and Sons, Inc., 1992

Bliss, J. and Stevenson, D. W., "Fiber Optics: A Designer's Guide to System Budgeting," *Electro-Opt. Sys. Design*, **13**, 23-32, Aug. 1981

Botez, D., Ettenburg, "Comparison of Surface and Edge Emitting LED for Use in Fiber Optical Communications," *IEEE Trans. Electron Devices*, **ED-26**, 1230-1238, Aug. 1979

Brininstool, M. R., "104-km Unrepeatered Bidirectional Fiber Optic Demonstration Link," Naval Oceans System Center Technical Report 1185, May 1987

Dyott, R. B. and Stern, J. R., "Group Delay in Glass Fiber Waveguide," *Electron. Lett.*, **7**, 82-84, Feb. 1971

Gambling, W. A., Matsumara, H., and Ragdale, C. M., "Mode Dispersion, Material Dispersion, and Profile Dispersion in Graded Index Single Mode Fibers," *Microwaves, Opt., and Acoustics*, **3**, 239-246, Nov. 1979

Hewlett Packard Company, Fiber Optics Handbook, Hewlett Packard Company, 1989

IEEE Standard 812-1984, IEEE Standard Definitions of Terms Relating to Fiber Optics, The Institute of Electrical and Electronics Engineers, New York, 1984

Ishio, H., Minowa, I., and Nosu, K., "Review and Status of Wavelength Division Multiplexing Technology and its Application," *IEEE Journal of Lightwave Technology*, **LT-2**, 448-463, Aug. 1984

Ito, K., Umeda, Y., Sugiyama, Y., Nakajima, K., Oshima, K., and Nunoshita, M., "Bidirectional Fibre Optic Loop-structured Network," *Electron. Lett.*, **17**, 84-86, Jan. 1981

Jacobs, I., "Design Considerations for Long-haul Lightwave Systems," *IEEE Journal on Selected Areas in Communications*, **SAC-4**, 1389-1895, Dec. 1986

JDS Optics, measured data sheet for WD1415 series WDMs, Feb. 1991

Kawana, A., Miya, T., Imoto, N., and Tsuchiya, H., "Pulse Broadening in Long-span Dispersion-free Single-mode Fibers at 1.5 $\mu$m," *Electron. Lett.*, **16**, 188-189, 28 Feb. 1980

Keiser, G., Optical Fiber Communications, McGraw-Hill Inc., 1983

Killen, H. B., Fiber Optic Communications, Prentice Hall, Inc., 1991

Lacy, E. A., Fiber Optics, Prentice Hall, Inc., 1982

Laser Diode Inc., measured data sheet for LDDL 2510 and LDDL 2515 transmitter/ receiver, 1990

Miller, S. E., Marcatili, E. A. J., and Li, T., "Research Toward Optical Fiber Transmission Systems," *Proc. IEEE*, **61**, 1703-1751, Dec. 1973

OFTI, connector data sheet for STC-type fiber optic connectors, 1987

Palais, J. C., Fiber Optic Communications, Prentice Hall, Inc., 1988

Rupp Corporation, Fastlynx User's Manual Version 1.0, Sewell Development Corporation, 1989

Sanders, L., "Single-chip Encoder-Decoder Converts NRZ into Manchester Code," *Electronics*, 105-109, 28 July 1982

Sterling, D. J., Technician's Guide to Fiber Optics, Delmar Publishers Inc., 1987

Sugimoto, S., Minemura, K., Kobayashi, K., Seki, M., Shikada, M., Ueki, A., Yanase, T., and Miki, T., "High-speed Digital-signal Transmission Experiments by Optical WDM," *Electron. Lett.*, **13**, 680-682, Oct. 1977

Van Etten, W., Van der Platts, J., Fundamentals of Optical Fiber Communications, Prentice Hall International (UK) Ltd., 1991

Weik, M. H., Fiber Optics Standard Dictionary, Van Nostrand Reinhold, 1989

White, K. I. and Nelson, B. P., "Zero Total Dispersion in Step Index Monomode Fibers at 1.30 and 1.55 $\mu$m," *Electron. Lett.*, **15**, 396-397, June 1979